Cleaner Engineering and Technology 23 (2024) 100818

Contents lists available at ScienceDirect

Cleaner Engineering and Technology

journal homepage: www.sciencedirect.com/journal/cleaner-engineering-and-technology

Summer period analysis of the rotary desiccant - hybrid cooling system combined with solid oxide fuel cells using human waste fuel

Kamil Neyfel Çerçi [a,b,*], Ivo Rafael Oliveira Silva [c], Önder Kaşka [d], Kamel Hooman [a,**]

[a] Department of Process and Energy, Delft University of Technology, Leeghwaterstraat 39, 2628CB, Delft, the Netherlands
[b] Tarsus University, Faculty of Engineering, Department of Mechanical Engineering, 33400, Tarsus, Mersin, Turkiye
[c] University of Coimbra, Faculty of Science and Technology, Department of Mechanical Engineering, 3030-788, Coimbra, Portugal
[d] Osmaniye Korkut Ata University, Faculty of Engineering, Department of Mechanical Engineering, 80000, Osmaniye, Turkiye

ARTICLE INFO

Keywords:
Desiccant wheel
Vapor compression cooling
Solid oxide fuel cells
Human waste
Biomass
Refrigerants

ABSTRACT

This paper proposes and simulates a desiccant air cooling system integrated with a vapor compression cooling unit and a heat recovery unit for an office building in Çanakkale, Turkey, during the summer season. The required electrical energy for equipment of the proposed system is supplied by an Solid Oxide Fuel Cells (SOFC) unit using human waste as fuel. Moreover, some of the waste heat generated by the SOFC is used to regenerate the desiccant wheel. The simulation also includes the effects of three different refrigerants for the vapor compression cooling unit. Among the refrigerants, the highest electrical COP was obtained for the system using R1234ze(Z), which is 3.14% and 2.40% higher than the systems using R717 and R1233zd(E), respectively. Additionally, the system using R1234ze(Z) achieved electrical savings of 9.97% and 9.23% compared to the other systems. These electrical savings resulted in fuel savings of 1.19% and 0.90% for R1234ze(Z) compared to R717 and R1233zd(E), respectively. During the summer season, the electricity production from the existing SOFC unit met 82.00% of the total electricity consumption of the desiccant hybrid cooling system. Furthermore, a difference of 3984.56 kWh in primary energy consumption was identified between the desiccant hybrid cooling systems operating with the SOFC and without the SOFC during the summer season.

1. Introduction

The building sector accounts for approximately 40% of total energy consumption of the world, with 50–70% of this energy usage attributed to climate control systems (Masoso and Grobler, 2010; Omer, 2008). As countries become more developed, the growing demand for comfort conditions in buildings has significantly increased the market for space cooling applications worldwide (Jani et al., 2018; Sheng et al., 2015). In the ever-evolving competitive environment, there is a constant search for solutions to reduce energy consumption in buildings and alleviate the pressure of the global energy resource shortage (Daou et al., 2006).

In hot and humid regions, achieving comfort conditions in buildings requires not only reducing the temperature of the outdoor air but also its humidity (Heidari et al., 2019). Currently, cooling and dehumidification processes are typically achieved using vapor compression cooling systems (Delfani et al., 2010). The traditional vapor compression cooling systems are considered insufficient for providing the desired comfort conditions in hot and humid regions due to the excessive cooling or unnecessary reheating costs. One efficient dehumidification method is the use of special outdoor air systems with desiccants that remove moisture through sorption (Frein et al., 2018). Typically, compact, less corrosive, and continuously operable rotary solid desiccants (DW) are more popular and widely used in buildings (Jia et al., 2006; Tu et al., 2014). However, these systems are limited by local energy distribution, system structure, initial investment or operating costs, climate, and regional factors. Additionally, as the amount of moisture removal from the process air increases, the energy required for regeneration heat also increases, leading to a higher sensible heat load that needs to be removed from the system. To overcome these two main challenges, many researchers have utilized solar energy, one of the alternative energy sources, to meet the regeneration heat. The most widely used solar energy technology for this purpose is solar collectors (Chen et al., 2022; Tian et al., 2020). In recent years, interest has also increased in the use of photovoltaic (PV) and photovoltaic thermal (PVT) panels in these

* Corresponding author. Department of Process and Energy, Delft University of Technology, Leeghwaterstraat 39, 2628CB, Delft, the Netherlands.
** Corresponding author.
E-mail addresses: K.N.C.Cerci@tudelft.nl, kneyfelcerci@tarsus.edu.tr (K.N. Çerçi), K.Hooman@tudelft.nl (K. Hooman).

https://doi.org/10.1016/j.clet.2024.100818
Received 30 July 2024; Received in revised form 11 September 2024; Accepted 7 October 2024
Available online 11 October 2024

systems (Guo et al., 2020; Lo Basso et al., 2021). Lo Basso et al. (2021) simulated a trans-critical CO_2 heat pump integrated with a desiccant cooling system for reducing the contribution of external thermal sources. The electrical COP was found as 0.9 for Milan, 1.75 for Rome, and 1.78 for Palermo and thermal COP was 0.36 for Milan, 0.61 for Rome and Palermo for the hybrid system. Olmuş et al. (2023) simulated a solid desiccant air conditioning system for a building in Adana, Turkey, during entire cooling season. The electrical and thermal energy required for the proposed system is provided by water-cooled PV/T units. The results showed that the proposed air conditioning system is a self-sustaining and sustainable system.

A study presented by researchers from the National Renewable Energy Laboratory (NREL), a research unit of the U.S. Department of Energy, highlighted two major barriers to the sustainable application of solar energy technologies in cooling technologies (Odukomaiya et al., 2021). These are the inability to meet 100% of the electricity required for cooling applications with solar energy technologies and the need for very large facilities to meet the cooling demand with solar energy. The limitations necessitate the development of more sustainable alternative energy technologies compared to solar energy applications in cooling systems. One of these alternative technologies is the use of solid oxide fuel cells (SOFC) in rotary desiccant cooling systems. SOFCs are one of the next-generation power generation technologies due to their excellent energy conversion performance and low environmental emissions (Haseli, 2018; Roushenas et al., 2020). The use of SOFC technology in rotary desiccant cooling systems is quite limited in the literature. Fong and Lee (2019) performed performance analyses of a small-capacity SOFC-assisted rotary desiccant cooling system that can be utilized for 24 h. In the system, the waste heat generated by the SOFC unit was used to meet the regeneration heat of the DAC system. The electricity produced by the SOFC was used to meet the building's electricity needs. The researchers also emphasized that such a system has high potential for sustainable application in the future. However, in this system, natural gas was used as the fuel to operate the SOFC unit. The major drawback of natural gas is that it is a non-renewable energy source and therefore not a sustainable energy source for the future (Naqvi et al., 2018). In this context, the use and development of renewable energy to meet energy needs has become one of the main research focuses today (Islam et al., 2019). Among all renewable energy sources, biomass energy is the fourth largest energy source in the world, accounting for approximately 14% of the world's primary energy demand (Dong et al., 2009). Therefore, the clean and efficient use of biomass energy has become a significant topic in the renewable energy field. Thus, the integration of biomass gasification and SOFC is expected to achieve the goal of clean and efficient energy conversion (AlNouss et al., 2020; Cavalli et al., 2021).

One of the applications of rotary desiccant cooling systems is the combination of a desiccant wheel and a vapor compression heat pump, which can be used widely and efficiently without any limitations (Sheng et al., 2013, 2014). However, these systems also have some drawbacks such as higher electricity demand because of compressor power consumption, the need for an additional heater to meet the required regeneration heat and low COPs due to the higher temperature difference between the condenser and the evaporator. Combining SOFC units, which use biogas as a renewable energy source and have the potential to produce waste heat during electricity generation, with desiccant hybrid cooling systems offers a solution to these shortcomings of the current heat pump-assisted desiccant cooling systems.

In this study, for the first time, the effects of using a self-sustainable SOFC unit fueled by human waste (Liu et al., 2014) in combination with a desiccant hybrid cooling system were analyzed. The analyses were conducted for a 60 m^2 office considering the climatic conditions of Çanakkale, Turkey, during the summer season. The effects of three different refrigerants (R717, R1233zd(E), and R1234ze(Z)) on performance and electricity consumption of the system, as well as the implications of these effects on SOFC capacity, fuel consumption, and the disposal of solid waste from the environment, were also investigated. The theoretical results obtained from this study are expected to inspire many researchers in using different types of biogas-fueled SOFC units to meet the energy needs of desiccant cooling systems and to explore new research avenues to make this use more sustainable.

2. System description

The proposed system consists of four subsystems: a solid oxide fuel cell unit (SOFC), a thermal energy storage unit (TES), a desiccant air-cooling unit (DAC), and a vapor compression cooling unit (VCC) (Fig. 1). In the DAC unit, outdoor air (fresh air) is first sucked into the process air duct by a fan (1 → 2). The high humidity outdoor air enters the rotary desiccant wheel (DW) in the process air duct and exits at a lower humidity and higher temperature (2 → 3). The process air then passes sequentially through heat exchangers (rotary heat exchanger-RHX and evaporator) to achieve the desired air conditions (3 → 5). In this system, the exhaust air from the indoor environment, which has relatively lower humidity compared to the outdoor air, is directly used for regeneration air. First, the regeneration air passes through the RHX to recover some heat from the process air (7 → 8). Then, the regeneration air is heated to the required regeneration air temperatures using the waste heat from the condenser (8 → 9). However, if the amount of heat from the condenser is insufficient to reach the required regeneration air temperatures, part or all of the waste heat produced by the SOFC is used for this process (9 → 10).

The SOFC unit is primarily used to supply the electrical energy required by the system. While generating electricity, the SOFC unit also produces a significant amount of waste heat. While a portion of this waste heat is stored in the TES unit (20 → 19), another portion is used to provide the regeneration heat needed by the desiccant hybrid cooling system (17 → 18).

The VCC unit consists of four main components: the evaporator, compressor, condenser, and expansion valve. In this unit, the evaporator absorbs heat from the process air, causing the working fluid circulating in the VCC cycle to evaporate (15 → 12). The working fluid then enters the compressor, where its pressure and temperature increase (12 → 13). The high-pressure, high-temperature working fluid enters the condenser to release its heat to the regeneration air and condenses (13 → 14). Finally, pressure and temperature of the working fluid are reduced by the expansion valve, allowing it to return to the evaporator conditions (14 → 15).

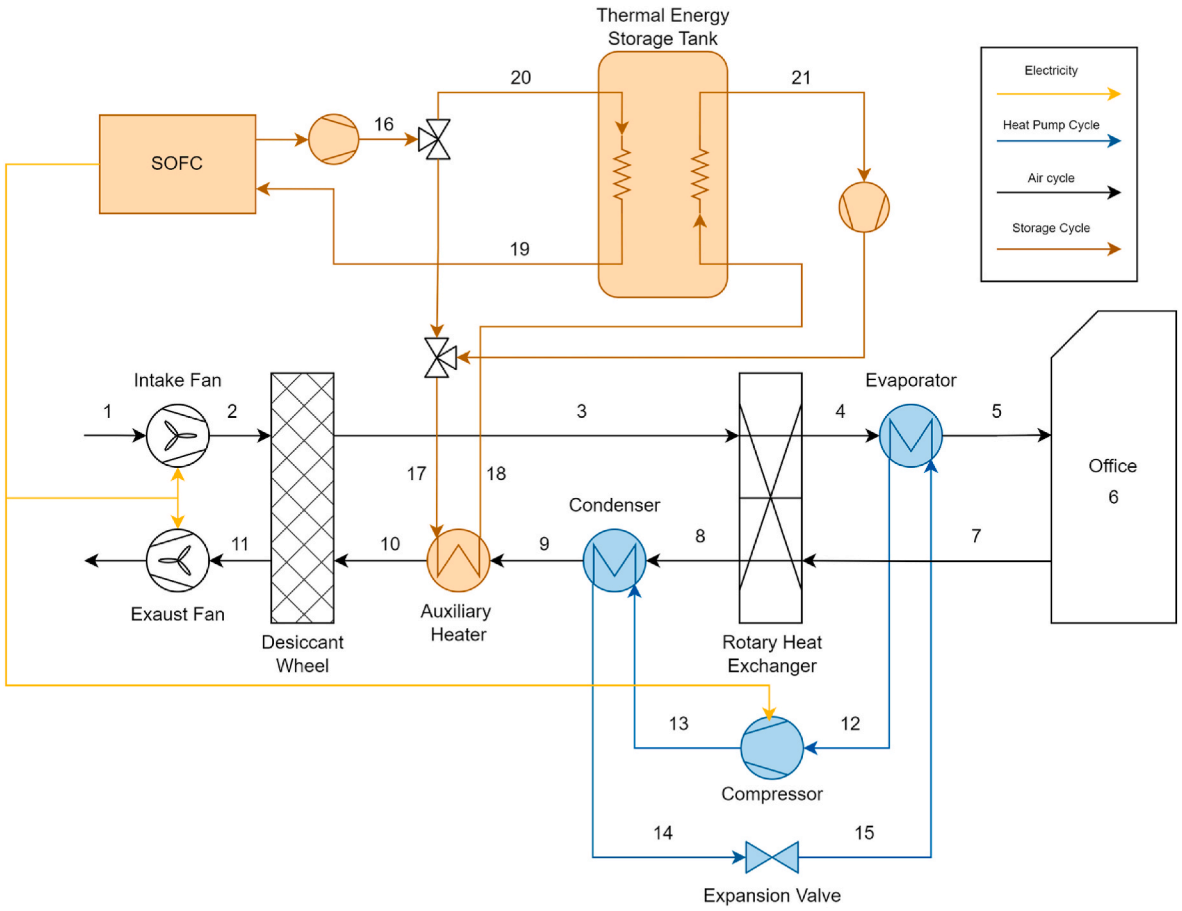

Fig. 1. Schematic view of the proposed system
1: outdoor ambient air conditions8: regeneration air entering the condenser15: refrigerant entering the evaporator
2: process air entering the DW9: regeneration air entering the auxiliary heater 16: waste heat from SOFC
3: process air entering the RHX 10: regeneration air entering the DW17: water entering the auxiliary heater
4: process air entering the evaporator 11: regeneration air from the DW18: water from the auxiliary heater
5: process air entering the office room12: refrigerant entering the compressor19: outlet from TES unit in charged process
6: indoor ambient air conditions13: refrigerant entering the condenser20: inlet to TES unit in charged process
7: regeneration air entering the RHX14: refrigerant entering the expansion valve21: outlet from TES unit in discharged process.

3. Modelling

A detailed analysis of the proposed desiccant hybrid cooling system was conducted based on weather data for the summer period. Simulations were performed for the cooling season, which includes June, July, and August, considering office hours (from 8:00 to 17:00). Outdoor air and desired indoor air conditions are crucial parameters for cooling load of the office building. In this study, an office building with a gross area of 60 m^2 was considered, and a dry-bulb temperature of 26 °C was chosen for the indoor condition. The climate data for Çanakkale, Turkey, were obtained using TRNSYS software (Meteonorm data) (Fig. 2) (Klein, 2017). Building construction materials and design loads were selected according to Turkish Standard 825 (TS-825, 2013) and ASHRAE 90.1 (Goel et al., 2017), respectively. Table 1 summarizes the main input data for cooling load calculations. Cooling loads were obtained using EnergyPlus software and are presented in Fig. 3 (Crawley et al., 2000). The total cooling load was the lowest in June at 251.95 kWh and the highest in July at 511.07 kWh.

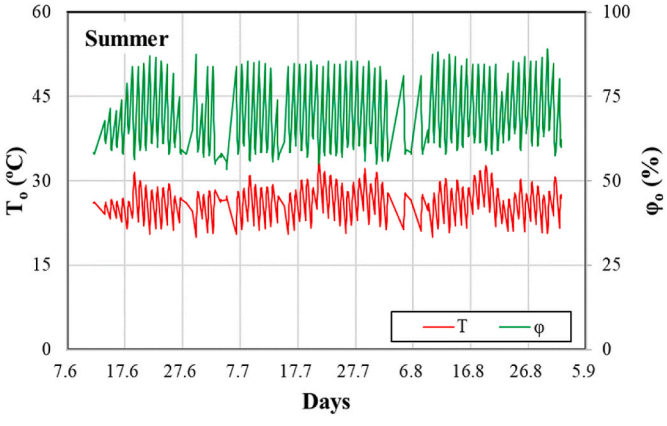

Fig. 2. Hourly variation of ambient air dry-bulb temperature, relative humidity for Çanakkale.

Table 1
The main input data for cooling load calculations.

Parameter	Value	Units
Roof U-Value	0.48	W/m^{2}K
Ground U-Value	0.30	W/m^{2}K
External Wall U-Value	0.32	W/m^{2}K
Windows U-Value	2.7	W/m^{2}K
Doors U-Value	0.070	W/m^{2}K
Occupancy	18.6	m^2/person

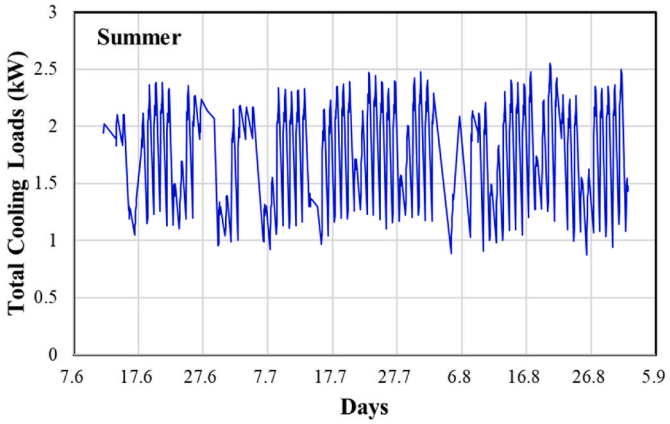

Fig. 3. Total cooling load of the office building for the months of summer season.

3.1. System formulations

Many researchers have developed models to account for the effects of various parameters in order to calculate the output conditions of desiccant wheel (DW) (Motaghian et al., 2021; Zendehboudi and Li, 2018). In this study, the multiple linear regression model developed by Güzelel et al. (2021) for balanced flow was used. This model has higher accurately predicts for output temperature and humidity of DW in process air channel, making it a preferred choice in various simulation studies (Çerçi et al., 2024; Olmuş et al., 2023). More detailed information on the use of the model can be found in the literature (Çerçi et al., 2024; Güzelel et al., 2021). Silica gel was selected as the desiccant material, the dimensions of the DW were assumed to be 440 mm × 200 mm with a rotation speed of 12 rev/h. Additionally, energy and mass balance equations were used to calculate the regeneration air conditions exiting the DW (**Eqs. 1 and 2**) (Güzelel et al., 2022).

$$\dot{m}_2(\omega_2-\omega_3)=\dot{m}_{10}(\omega_{11}-\omega_{10}) \tag{1}$$

$$\dot{m}_2(h_3-h_2)=\dot{m}_{10}(h_{10}-h_{11}) \tag{2}$$

To reduce the cooling load on the evaporator, a gas-to-gas rotary-type heat exchanger was used (Kays and London, 1984);

$$\dot{Q}_{RHX}=\dot{m}_3c_{p,3}(T_3-T_4)=\dot{m}_7c_{p,7}(T_8-T_7) \tag{3}$$

$$\dot{Q}_{RHX}=\varepsilon_{RHX}\dot{Q}_{max,RHX} \tag{4}$$

Where, ε_{RHX} was assumed to be 0.85 in this study (Song and Sobhani, 2020). The efficiency for the fans is assumed to be 0.8 (Çerçi et al., 2024; Tian et al., 2022). The maximum possible heat transfer rate was calculated using **Eq. (5)** (Kays and London, 1984).

$$\dot{Q}_{max,RHX}=C_{min,RHX}(T_3-T_7) \tag{5}$$

$$C_{min,RHX}=\dot{m}c_p \tag{6}$$

Where $C_{min,RHX}$ is the minimum of capacitance rate of hot and cold fluids. Both sensible and latent heat transfer occur in the evaporator to achieve comfort conditions (De Antonellis et al., 2012; Ozturk et al., 2020).

$$\dot{Q}_{e,s}=\dot{m}_4c_{p,4}(T_4-T_5) \tag{7}$$

$$\dot{Q}_{e,l}=\dot{m}_4h_{fg}(T_4-T_5) \tag{8}$$

$$\dot{Q}_e=\dot{Q}_{e,s}+\dot{Q}_{e,l} \tag{9}$$

It is assumed that there is 10 °C temperature difference between the evaporating temperature and the air exiting the evaporator to cool the process air, and 3 K temperature difference for superheating (Erdinc, 2023; Kutlu et al., 2019).

$$\dot{Q}_e=\dot{m}_{15}(h_{12}-h_{15}) \tag{10}$$

In this study, the desired dry bulb temperature of the indoor air was set to a constant value of $T_6 = 26$ °C, and the amount of air to be supplied to the building ($\dot{m}_5$) was calculated using **Eq. (11)**. Then, the indoor humidity ratio (ω_7) was obtained from **Eq. (13)** (Olmuş et al., 2023).

$$\dot{Q}_{c,t}=\dot{m}_5(h_6-h_5) \tag{11}$$

$$\dot{Q}_{c,sen}=\dot{m}_5c_{p,avg}(T_6-T_5) \tag{12}$$

$$\dot{Q}_{c,l}=\dot{m}_5h_{fg}(\omega_6-\omega_5) \tag{13}$$

It is assumed that the throttling process in the expansion valve, the other component of the VCC unit occurs isenthalpically ($h_{14} = h_{15}$) (Yilmaz and Erdinç, 2019). For calculating the compressor power consumption, the isentropic and mechanical efficiencies of the compressor were assumed to be 0.8 and 0.95, respectively (Ozturk et al., 2020).

$$\dot{W}_{comp}=\dot{m}_{12}(h_{13}-h_{12}) \tag{14}$$

$$\dot{W}_{comp,el}=\frac{\dot{W}_{comp}}{\eta_{is}\eta_{mec}} \tag{15}$$

Eqs. 16 and 17 were used to calculate the condenser load and the temperature of the air exiting the condenser. It was assumed that there is 10 °C temperature difference between the condensation temperature and the regeneration heat for the air exiting the condenser, and 3 K temperature difference for subcooling (Kutlu et al., 2019; Ozturk et al., 2020).

$$\dot{Q}_{cond}=\dot{m}_{13}(h_{13}-h_{14}) \tag{16}$$

$$\dot{Q}_{cond}=\dot{m}_8(h_9-h_8) \tag{17}$$

When the condenser load is insufficient to reach the required regeneration temperatures, an auxiliary heater is activated. **Eqs. 18 and 19** were used to determine the capacity of the auxiliary heater and the required hot water flow rate (Güzelel et al., 2022).

$$\dot{Q}_{req}=\dot{Q}_{RAH}-\dot{Q}_{cond} \tag{18}$$

$$\dot{Q}_{req}=\dot{m}_{16}c_{p,hw}(T_{17}-T_{18}) \tag{19}$$

Where, $\dot{Q}_{RAH}$ is the total amount of heat that needs to be transferred to the regeneration air from the condenser and the auxiliary heater, and it is calculated using **Eq. (20)**.

$$\dot{Q}_{RAH}=\dot{m}_8(h_{10}-h_8) \tag{20}$$

The total electricity consumption of the desiccant hybrid cooling system includes the compressor, fans, water pump, and other auxiliary equipment. The electricity consumption required by the system was supplied by the SOFC using human waste as fuel. In this study, a self-sustaining SOFC unit utilizing human waste as fuel, as described in

the literature, was used as a basis (Liu et al., 2014). The net electrical efficiency value ($\eta_{n,el}$ = 0.1168) was used to calculate the electricity produced by the SOFC unit for different processes. In addition to electricity generation, SOFC units also produce significant amounts of heat. The thermal efficiency value (η_h = 0.4499) was used to calculate the amount of waste heat produced by the SOFC unit. It was assumed that the maximum operating capacity of the SOFC is 8.84 kW, the same as the SOFC capacity studied by Liu et al. (2014). The amount of electricity ($\dot{W}_{n,e}$) generated by the SOFC for the cooling system and the required amount of syngas ($\dot{m}_s$) are presented in **Eqs. 21** and **22** (Liu et al., 2014).

$$\dot{W}_{n,el} = \dot{W}_{SOFC}\,\eta_{n,el} \tag{21}$$

$$\eta_{n,el} = \frac{\dot{W}_{SOFC}}{\dot{m}_s\,LHV_s} \tag{22}$$

where, LHVs is the lower heating value of the fuel, assumed to be 12.2 MJ/kg (Liu et al., 2014).

The amount of waste heat released during electricity generation by the SOFC was calculated using **Eq. (23)** (Kuo et al., 2020; Pan et al., 2022).

$$\dot{Q}_{h,r} = \dot{W}_{SOFC}\,\eta_h \tag{23}$$

The TES tank has a diameter of 1 m and a height of 1.9 m in simulations. The TES unit is considered a fully mixed water tank containing 1488 kg of water. In the analysis, it was assumed that the initial temperature of the water in the TES unit was 20 °C and that the flow control was managed to keep the temperature below 95 °C (Duffie and Beckman, 1980; Fong and Lee, 2019). The average temperature of the water in the TES unit was calculated using **Eq. (24)**.

$$T_w^+ = T_w + \frac{\Delta t}{(\dot{m}_w c_{p,w})}\left[\dot{Q}_{h,r} - \dot{Q}_{req} - (UA)_w(T_w - T_o)\right] \tag{24}$$

where T_w is the average temperature of the stored water (°C) in TES unit, T^+_w is the average temperature of the stored water in the next hour (°C) in TES unit, Δt is time difference (h), $\dot{m}_w$ is mass flow rate of water (kg/s), $c_{p,w}$ is specific heat capacity of water (J/kg°C), U is overall heat transfer coefficient (W/m^2°C), and A is heat transfer surface area (m^2).

The required solid waste during electricity generation by the SOFC was calculated using **Eq. (25)** (Kuo et al., 2020; Pan et al., 2022).

$$\eta_{p,g} = \frac{\dot{m}_s\,LHV_s}{\dot{m}_{s,w}\,LHV_{s,w} + \dot{W}_p} \tag{25}$$

where, $\eta_{p,g}$ is the efficiency of the plasma gasifier (0.5), $LHV_{s,w}$ is the lower heating value of the solid waste (19 MJ/kg), and $\dot{W}_p$ is the electrical energy consumed for plasma gasification.

3.2. Performance parameters

The performance parameters of the examined system include the ratio of the total building load to the thermal energy requirement (COP_{th}), the electrical energy requirement (COP_{el}) and the total performance coefficient (COP_t) in **Eqs. (26)–(28)** (Olmuş et al., 2023). Additionally, the dehumidification effectiveness, which is the performance indicator of the desiccant wheel, are calculated using **Eq. (29)** (Çerçi et al., 2024).

$$COP_{th} = \frac{\dot{Q}_{c,t}}{\dot{Q}_{RAH}} \tag{26}$$

$$COP_{el} = \frac{\dot{Q}_{c,t}}{\dot{E}_{req}} \tag{27}$$

$$COP_t = \frac{\dot{Q}_{c,t}}{\dot{Q}_{RAH} + \dot{E}_{req}} \tag{28}$$

$$\varepsilon_{DW} = \frac{\omega_2 - \omega_3}{\omega_2} \tag{29}$$

Where, $\dot{E}_{req}$ is the difference between the electrical energy requirement needed by the system and the electricity supplied to the system. The net thermal energy consumption of the system ($\dot{Q}_{aux}$) is calculated using **Eq. (30)**.

$$\dot{Q}_{RAH} = \dot{Q}^+ + \dot{Q}_{aux} \tag{30}$$

If heat production exceeds heat consumption, $\dot{Q}_{aux}$ will be negative. Since the cooling system requires both thermal and electrical energy, it is more appropriate to determine the primary energy consumption to evaluate the system's total energy consumption. The primary energy (PE) of the system is calculated using **Eq. (31)** (Fong et al., 2010).

$$PE = \frac{\dot{Q}_{aux}}{\eta_{th}} + \frac{\dot{E}_{req}}{\eta_{el}} \tag{31}$$

where, η_{th} and η_{el} are taken as 0.9 and 0.38, respectively.

4. Results and discussion

In this study, the performance parameters of a desiccant cooling system powered by a SOFC during the summer season were examined. The analysis assumed the integration of an existing SOFC unit, which uses human waste as fuel (Liu et al., 2014), into a desiccant hybrid cooling system. In the designed hybrid cooling system, the changes in the performance parameters of the cooling system and the required amount of syngas by the SOFC were determined for three different refrigerants (R717, R1233zd(E), and 1234ze(Z)), which have recently attracted the attention of many researchers. Additionally, the amount of solid waste (human waste) required to produce the syngas was also determined. The Engineering Equation Solver (EES) software, which can analyze by establishing a relationship between the thermophysical properties of humid air and the refrigerant, was used in the analyses (Klein, 2012).

4.1. Evaluation of system energy requirements during summer period

In Fig. 4, the total compressor power consumption and cooling load of the desiccant hybrid cooling system using different refrigerants during the summer season are presented. During June, the compressor power consumption was lower compared to the rest of the summer due to the lower cooling load. The highest compressor power consumption was on August 19, corresponding to the cooling load variations. The total compressor power consumption for the entire summer season with R1234ze(Z) was 507.60 kWh, which is 3.98% and 3.45% lower compared to the scenarios using R717 and R1233zd(E) refrigerants, respectively. Fig. 5 shows the comparison of the pressure-enthalpy (P-h) diagrams of the refrigerants for two different days with varying outdoor conditions (June 13 and August 19). Since the critical temperature of R1234ze(Z) is higher than that of R717, the compressor power consumption is lower. Additionally, the saturation slopes of R1234ze(Z) are steeper compared to those of R1233zd(E). This causes the refrigerant to enter the evaporator at lower qualities and higher heat transfer occurs throughout the evaporation process (via phase change). This explains why the compressor power consumption is lower when using R1234ze (Z) compared to R1233zd(E). Another notable result is that although the overall compressor power consumption with R1233zd(E) was slightly lower than with R717, on days with very high temperature and humidity ratio ($T_{outdoor} \geq 26$ °C and $\omega_{outdoor} \geq 16$ g_w/kg_{da}), the compressor power consumption with R1233zd(E) was slightly higher than with R717. As

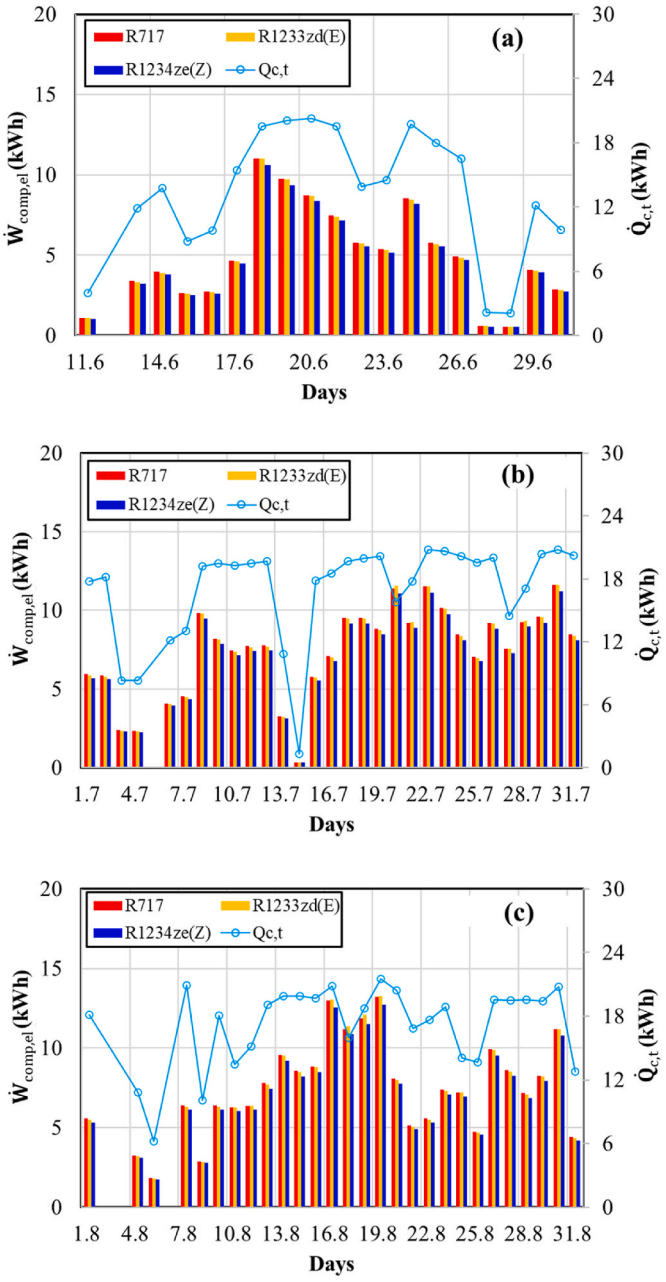

Fig. 4. Daily total compressor power consumption for June (a), July (b), and August (c) respectively.

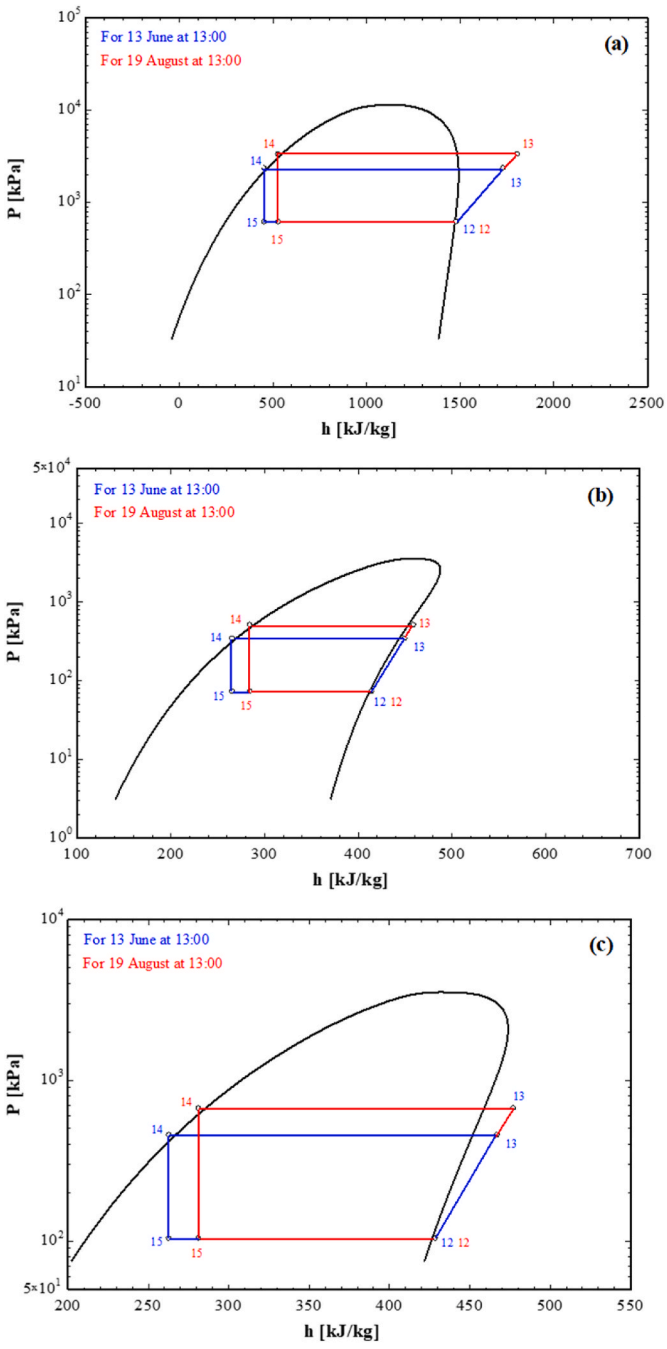

Fig. 5. The P-h charts for the use of R717 (a), R1233zd(E) (b), and R1234ze(Z) (c) refrigerants.

the ambient temperature and humidity rise, the temperature difference between the condenser and the evaporator also increases. When the temperature difference between the condenser and the evaporator exceeds 57.60 °C in the system using R1233zd(E) refrigerant, the performance parameters deteriorate compared to the desiccant hybrid cooling system using R717 refrigerant. The saturation slopes of R1233zd(E) are more horizontal compared to R717 (Fig. 5). Consequently, when the temperature difference between the evaporator and condenser exceeds 57.60 °C, the quality of the refrigerant entering the evaporator increases more for R1233zd(E) than for R717. This increase necessitates a higher mass flow rate of the refrigerant in R1233zd(E) compared to R717 to meet the same evaporator load. This rise in the mass flow rate of the refrigerant also results in a greater increase in compressor power consumption.

The condenser load varied proportionally with the compressor power consumption (Fig. 6). The highest condenser load was obtained

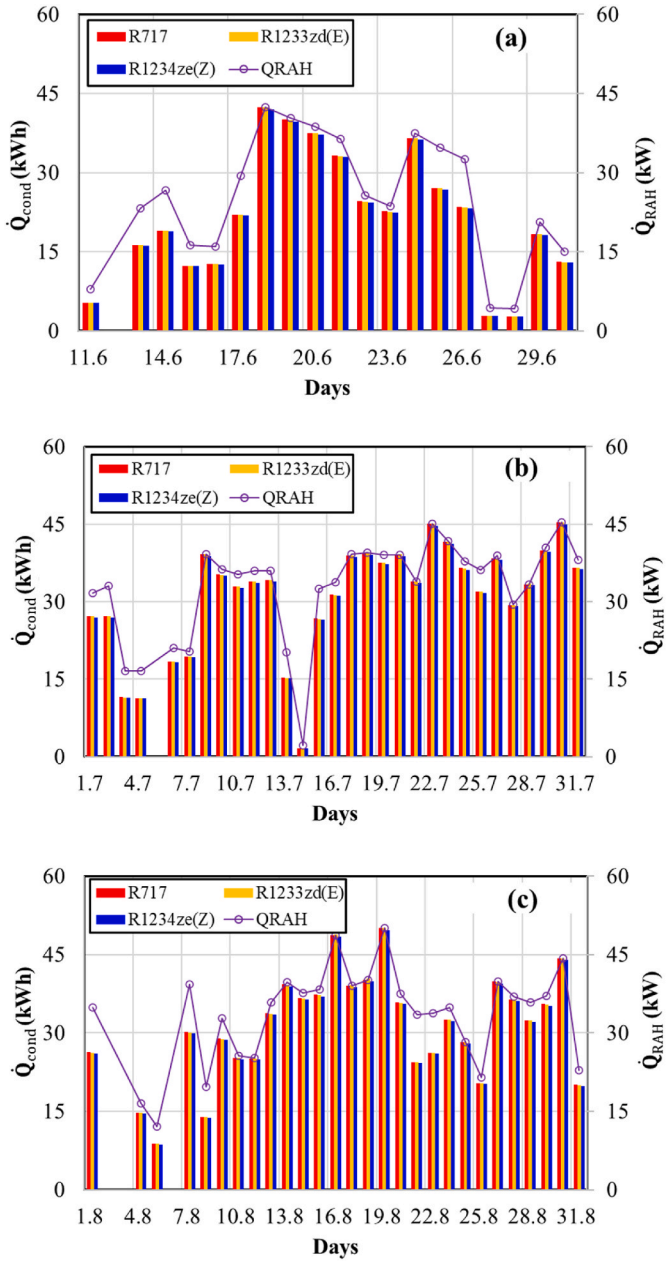

Fig. 6. Daily total condenser load for June (a), July (b), and August (c) respectively.

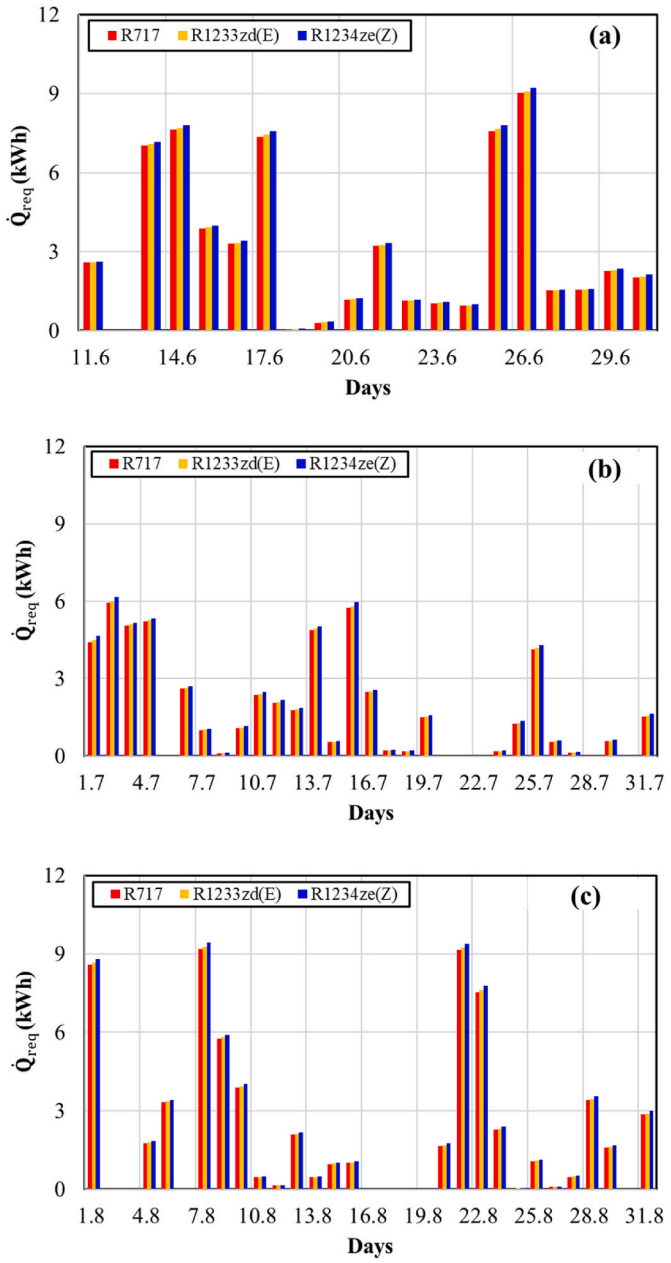

Fig. 7. Daily total heat requirement for June (a), July (b), and August (c) respectively.

for R717, which had the highest compressor power consumption, while the lowest condenser load was for R1234ze(Z), which had the lowest compressor power consumption. Due to the lower cooling load in June compared to other months, the heat rejected from the condenser was insufficient to meet the required Regeneration Air Heating (RAH) load (Figs. 4 and 6). On days with high cooling loads (mostly in the second half of July and mid-August), the amount of heat rejected from the condenser was sufficient to meet the required RAH load. On these days, the heat rejected from the condenser fully met the RAH load, eliminating the need for an auxiliary heater (Figs. 6 and 7). Throughout the cooling season in summer, the auxiliary heater wasn't needed for a total of 10 days.

Fig. 8 presents the total daily energy consumption of the proposed system. Since the total power consumption of the proposed system varied with the cooling load, it followed a trend similar to the total compressor power consumption (Figs. 4 and 8). The lowest power consumption was achieved by the cooling system using R1234ze(Z). The total power consumption for the cooling system using R1234ze(Z) during the summer season was found to be 704.60 kWh, which was 2.91% and 2.51% lower than the systems using R717 and R1233zd(E)

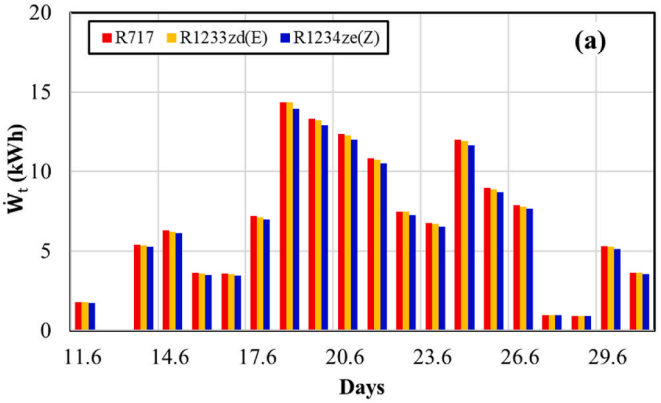

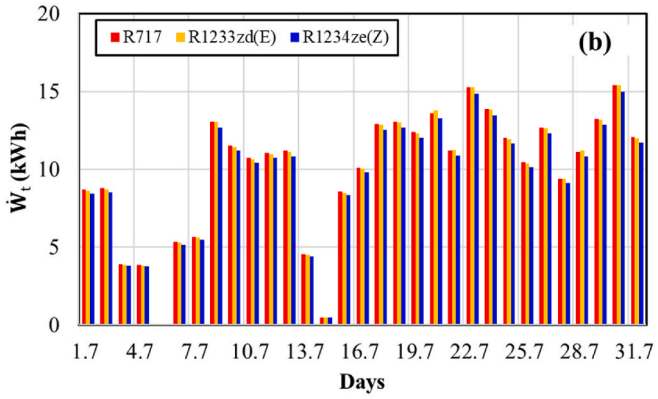

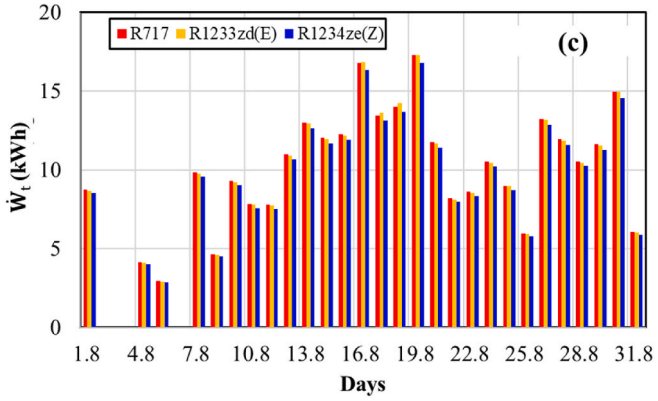

Fig. 8. Daily total electricity consumption for June (a), July (b), and August (c) respectively.

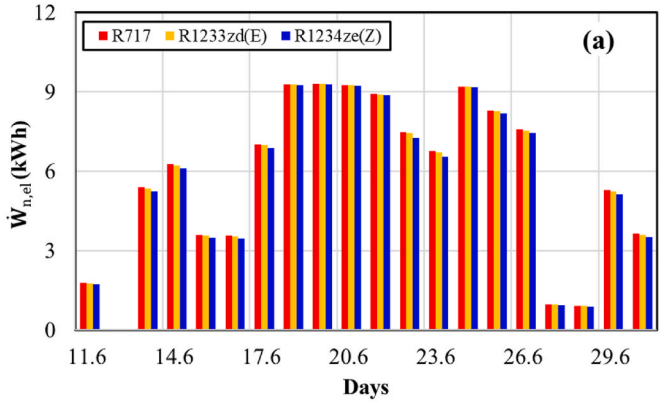

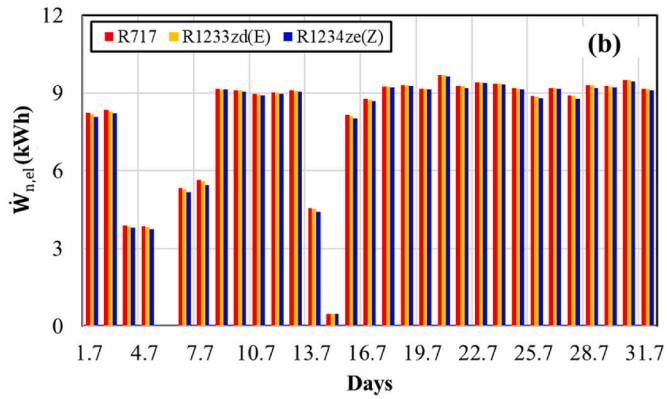

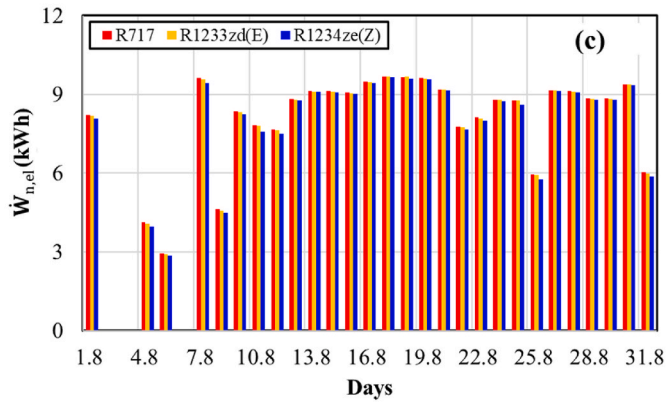

Fig. 9. Daily total net electricity production rate of SOFC for June (a), July (b), and August (c) respectively.

refrigerants, respectively.

4.2. Evaluation of energy production rates of SOFC during summer period

Fig. 9 presents the daily variation of the total net electric energy produced by the SOFC for use in the proposed system during the summer season. Since the proposed system with R1234ze(Z) had the lowest total energy consumption, it required the least amount of net electric energy production from the SOFC. The total electric energy produced for the proposed system with R1234ze(Z) reached a total of 577.10 kWh during summer period. This shows that during the summer period, the current electricity production of SOFC covered 82.00% of total electricity consumption of the cooling system. The remaining electricity demand, exceeding the capacity of the SOFC, was supplied from the electrical grid. Due to the higher energy consumption in systems using R717 and R1233zd(E), these systems required 1.20% and 0.90% more energy production, respectively, compared to the system with R1234ze(Z). The SOFC capacity required to meet the desired total daily electric production during summer period is shown in Fig. 10. The lowest SOFC capacity was obtained in June due to the lowest electricity demand, while

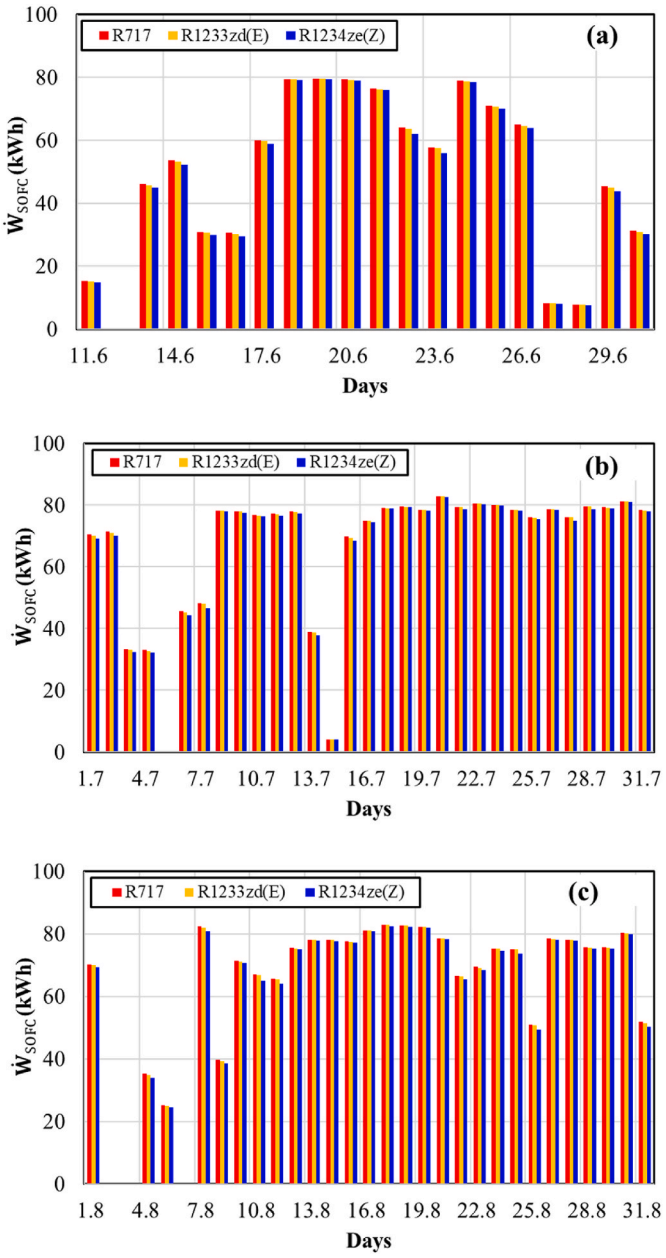

Fig. 10. Daily total SOFC capacity for June (a), July (b), and August (c) respectively.

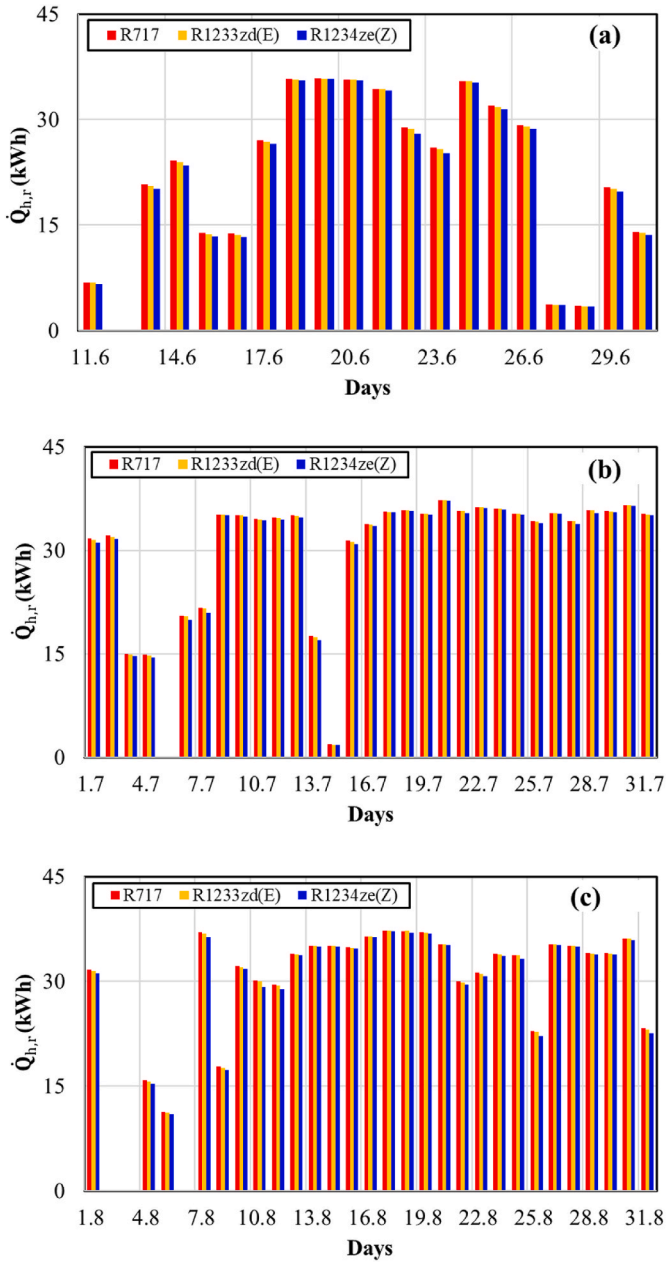

Fig. 11. Daily total heat recovered rate from SOFC for June (a), July (b), and August (c) respectively.

the highest SOFC capacity was needed in July (Fig. 10-a and b). A lower SOFC capacity was sufficient for the hybrid system using R1234ze(Z) compared to the others.

Significant amounts of waste heat are also generated during electricity production in SOFC units. During the summer, on days when the cooling load was low, the electricity demand met by the SOFC and the waste heat produced as a result were also lower compared to other days in the summer period. Nonetheless, the waste heat released from both the condenser and the SOFC was sufficient to meet the necessary regeneration air heating demand, and there was no need to activate an additional electric heater (Figs. 6 and 11). In the system using R1234ze (Z), the lower electric energy requirement led to less waste heat production.

4.3. Evaluation of the amount of fuel needed for SOFC and disposal of human waste during the summer period

The energy demand of the desiccant hybrid cooling system was met by the SOFC, which uses human waste as fuel. Fig. 12 exhibits the variation of the syngas needed to meet the SOFC capacity throughout the summer period. As mentioned in previous sections, the lowest syngas consumption occurred in June when the cooling load was lowest, and the highest syngas consumption occurred in July when the cooling load was highest. Due to the lowest energy consumption and SOFC capacity requirement, the lowest fuel consumption was observed in the hybrid system using R1234ze(Z). The total syngas consumed during the summer period was determined to be 12.63 t for R717, 12.59 t for R1233zd (E), and 12.48 t for R1234ze(Z).

To obtain syngas, the solid fuel undergoes a plasma gasification process. Therefore, this study also determined the amount of solid waste required to produce the desired syngas (Fig. 13). In June the solid waste

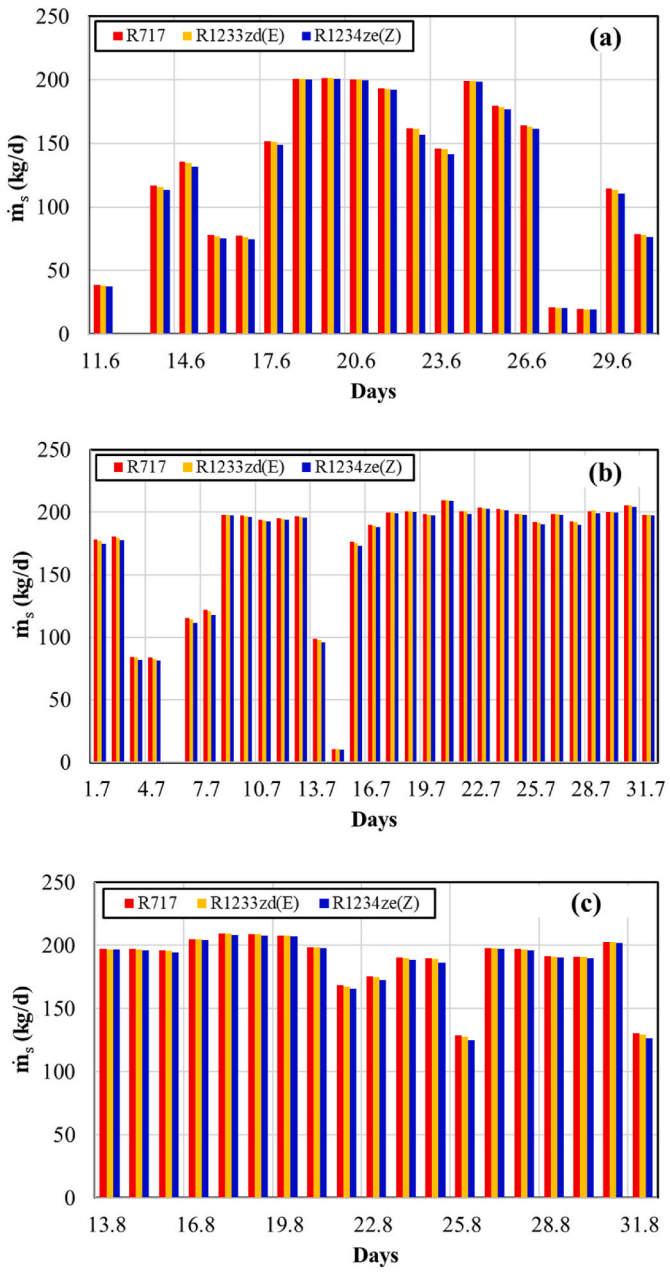

Fig. 12. Daily total syngas needed for SOFC for June (a), July (b), and August (c) respectively.

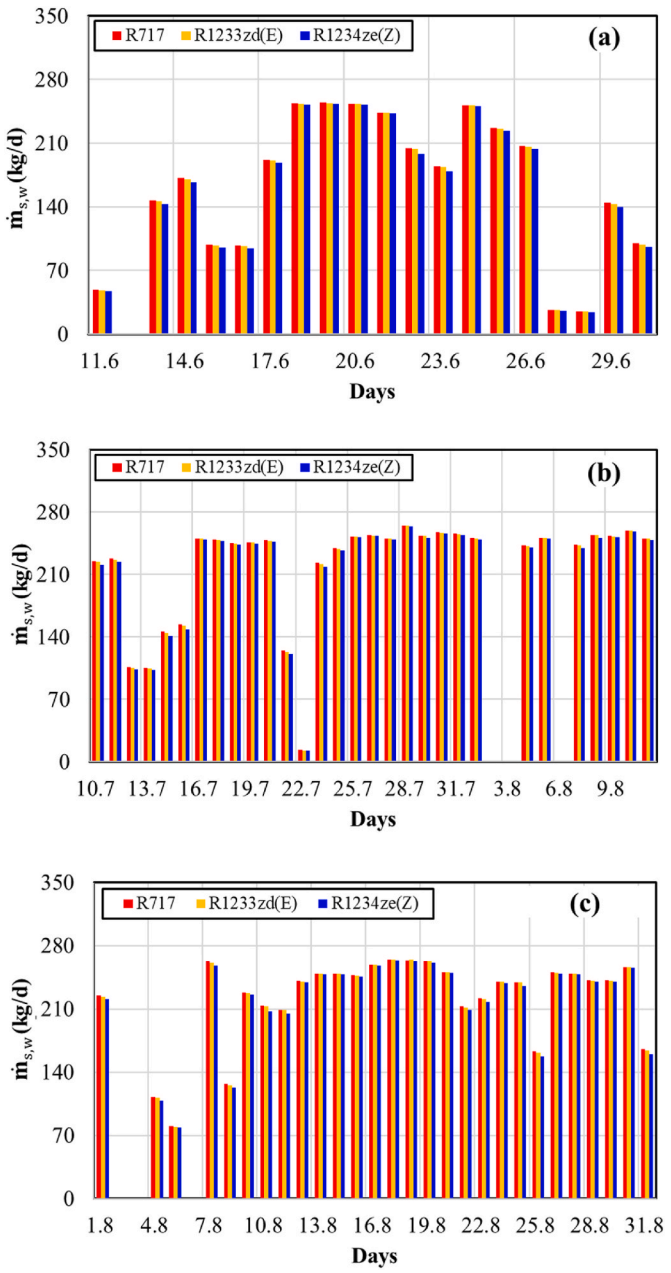

Fig. 13. Daily total solid waste needed for SOFC for June (a), July (b), and August (c) respectively.

requirement was also the lowest, while in July the solid waste requirement was the highest. During the summer period, in the case of using the refrigerant R1234ze(Z) the total solid waste requirement reached 15.77 t. This is 1.19% and 0.90% lower compared to the cases of using R717 and R1233zd(E), respectively. Therefore, due to the relatively lower fuel consumption requirement in R1234ze(Z), solid waste was used more efficiently.

4.4. Performance parameters of the system

Fig. 14 shows the variation of the COP_{el} of the desiccant hybrid cooling system throughout the summer period. The month with the highest COP_{el}, due to the lowest cooling load, is June. This is because the lowest electricity consumption occurred during this period. The average COP_{el} for R1234ze(Z) was 2.05, which is 3.14% and 2.40% higher than the systems using R717 and R1233zd(E), respectively. Higher COP_{th} was achieved at lower cooling loads, while lower COPth was obtained on

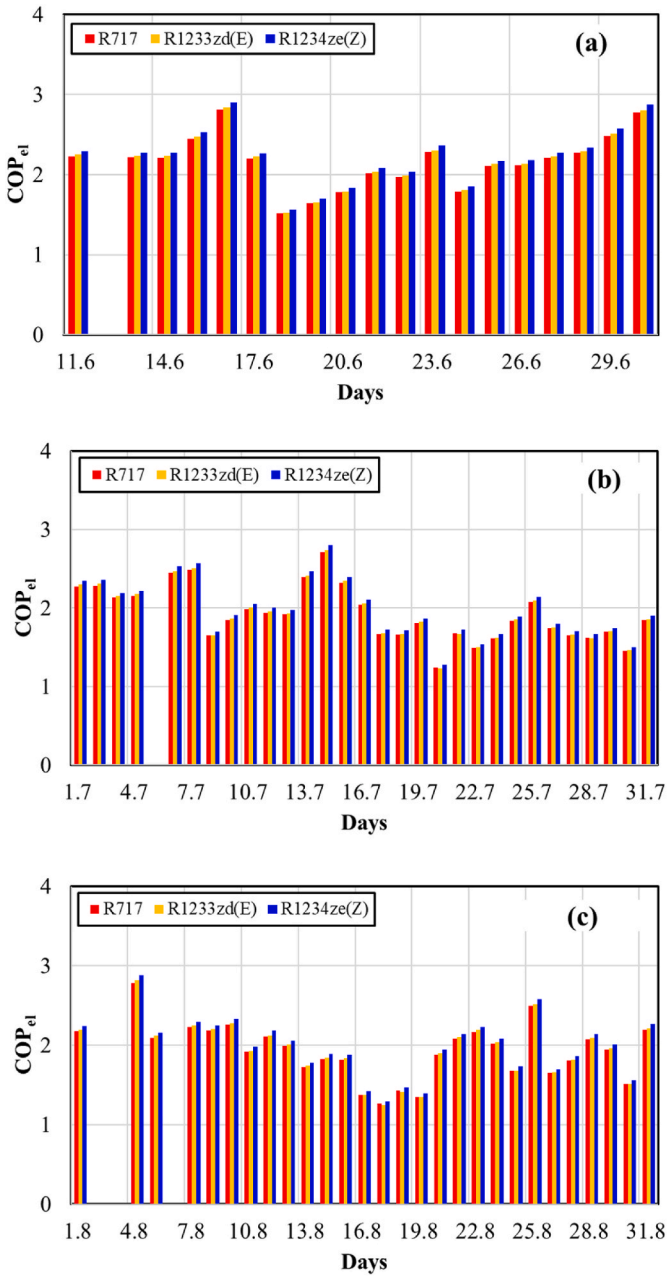

Fig. 14. Average COP_{el} of system for June (a), July (b), and August (c) respectively.

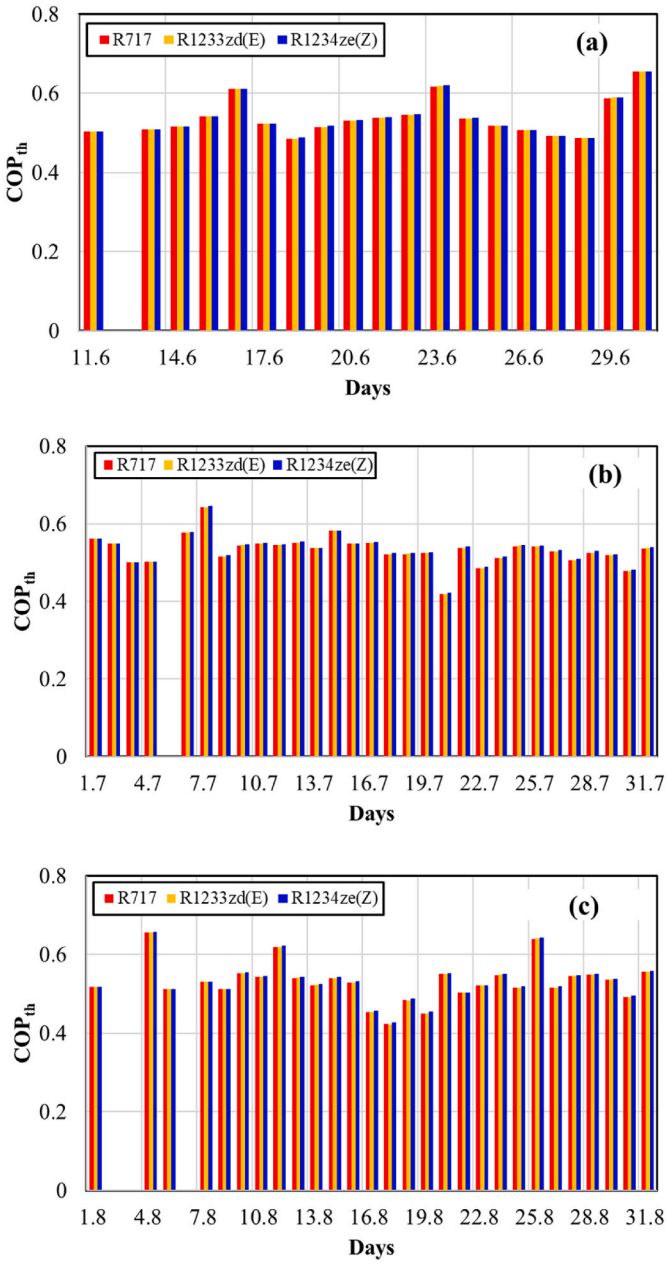

Fig. 15. Average COP_{th} of system for June (a), July (b), and August (c) respectively.

days with higher cooling loads (Fig. 15). For the system using the refrigerant R1234ze(Z), it was concluded that relatively lower regeneration air temperatures were sufficient, leading to relatively higher COP_{th} and the average COP_{th} was 0.53. According to the variation of the COP_t performance parameter, it was found that, similar to the previous performance parameters, high values were obtained on days with low cooling loads, and low values were obtained on days with high cooling loads (Fig. 16). Like the other performance parameters, the highest COP_t was obtained for the cases using the refrigerant R1234ze(Z) and the average was 0.42 for COP_t. In Fig. 17, the variation of the ε_{DW}, which represents the dehumidification performance of the DW, one of the system's most important components, and the cooling load throughout the summer period is presented. The cooling load generally varies in direct proportion to the outdoor temperature and humidity. When the cooling load increased, the ε_{DW} decreased, and when the cooling load

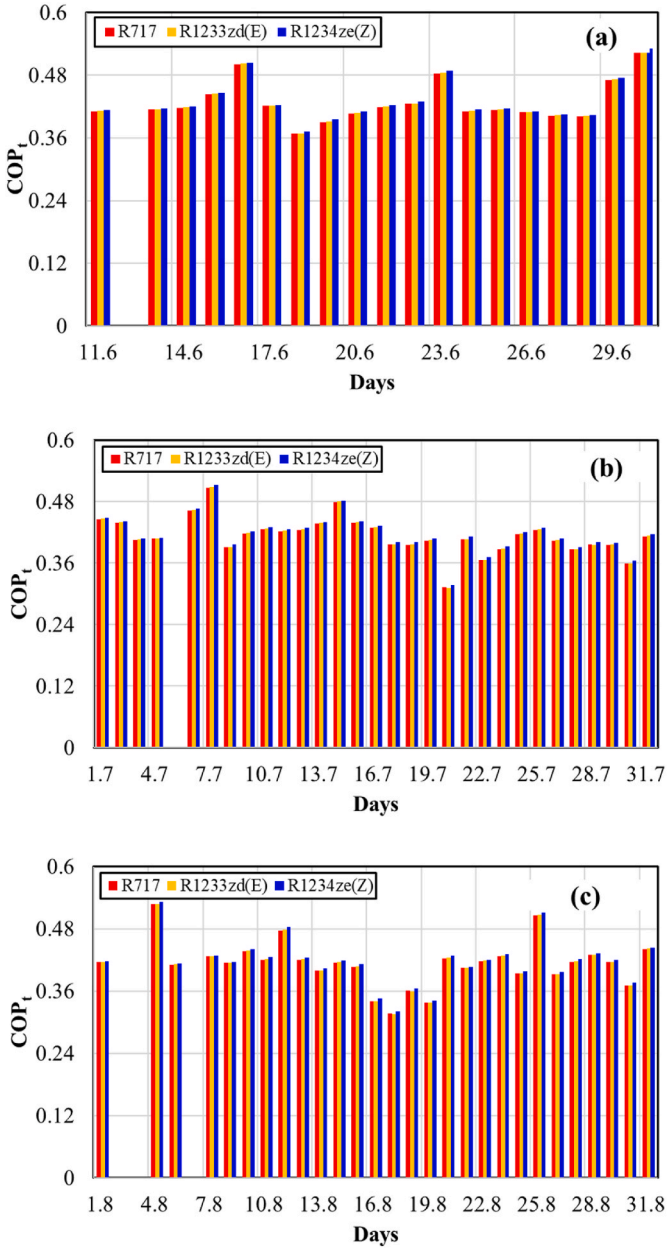

Fig. 16. Average COP_t of system for June (a), July (b), and August (c) respectively.

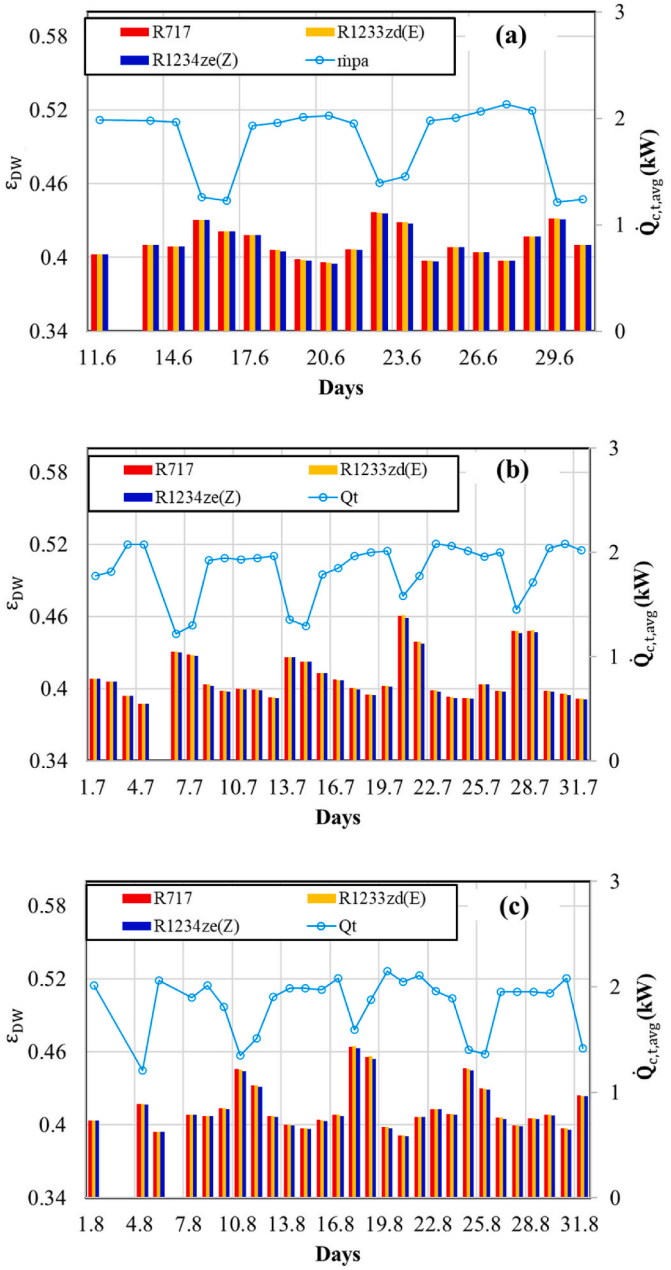

Fig. 17. Average dehumidification effectiveness and cooling load of system for June (a), July (b), and August (c) respectively.

decreased, the ε_{DW} increased. This indicates that the cooling load and the outdoor temperature and humidity, which the cooling load depends on, have an effect on ε_{DW}. The use of refrigerants had very little impact on ε_{DW}, and the lowest ε_{DW} values were obtained for R1234ze(Z). For R1234ze(Z), the lowest compressor power consumption and consequently the lowest condenser capacity were achieved (Figs. 4 and 6). This resulted in lower regeneration heat being released, leading to reduced moisture transfer in the DW where lower regeneration heat was applied.

4.5. Primary energy consumption

In some part of June, it is observed that the electricity generated by the existing SOFC is mostly sufficient for the desiccant hybrid cooling system (Fig. 18). However, for most of the remaining summer days, the electricity demand exceeds the capacity of the existing SOFC unit, necessitating additional electricity from the grid. During the summer period, the system using the refrigerant R1234ze(Z), which has the

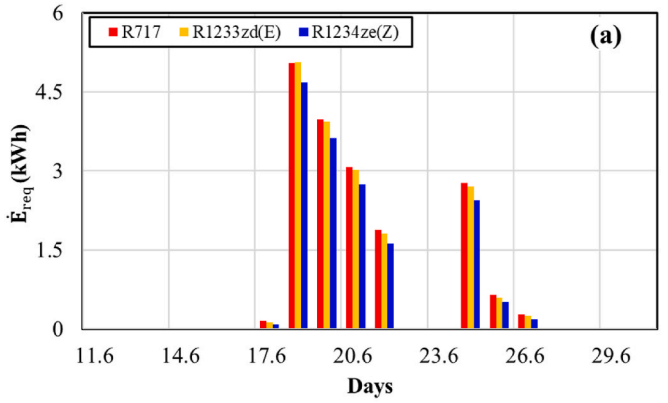

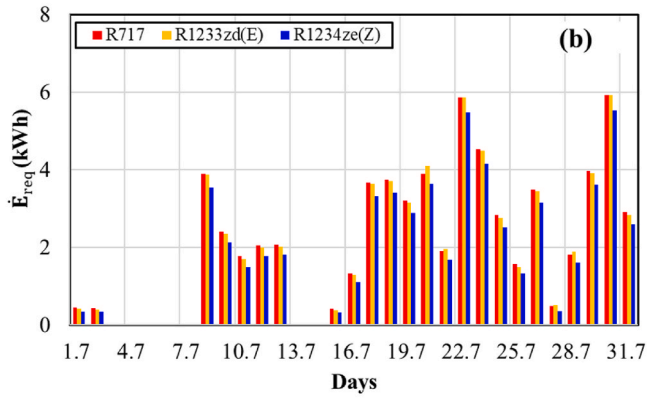

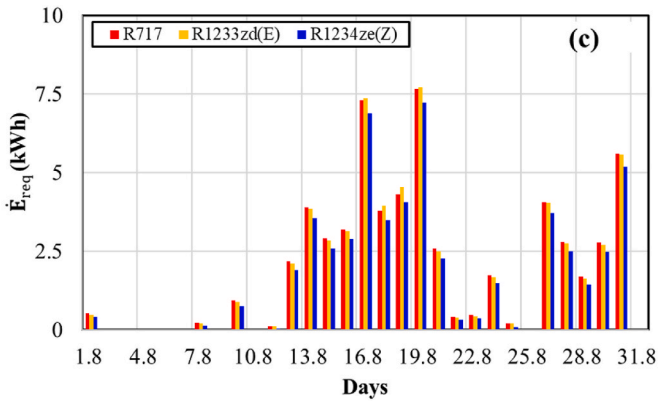

Fig. 18. Daily total electricity needed for desiccant hybrid cooling system for June (a), July (b), and August (c) respectively.

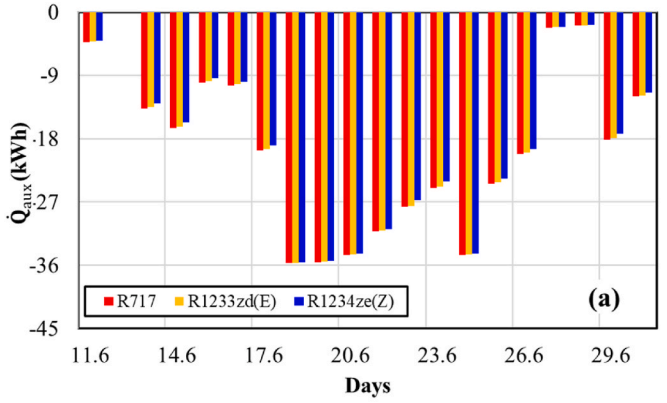

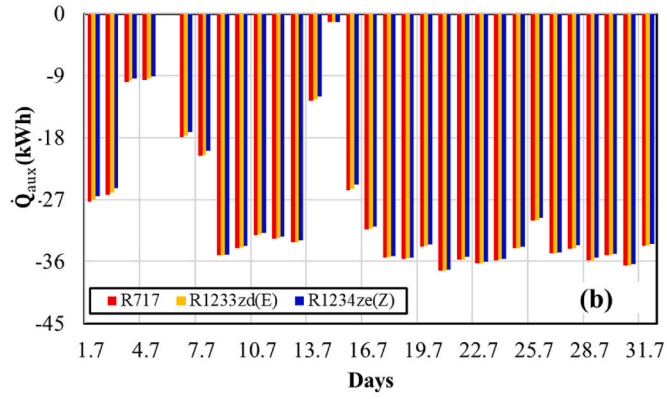

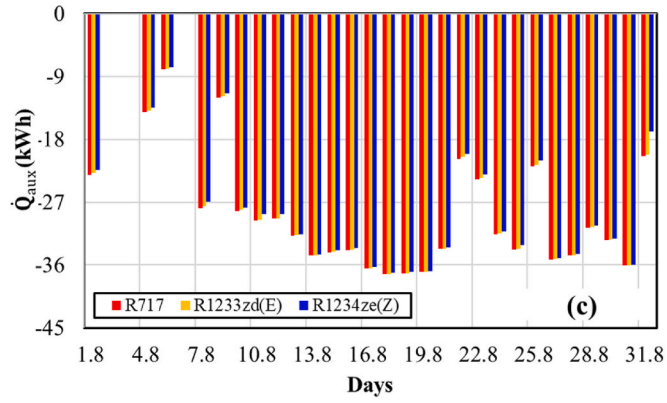

Fig. 19. Daily total heat needed for desiccant hybrid cooling system for June (a), July (b), and August (c) respectively.

lowest energy consumption, requires the least additional electricity. This results in a savings of 9.97% and 9.23% in additional electricity compared to the systems using R717 and R1233zd(E), respectively.

It is clearly evident that there is excessive heat production on days when cooling is needed during the summer months (Fig. 19). The primary purpose of the SOFC unit is to generate electricity. However, while producing electricity, the SOFC also generates a significant amount of waste heat. The analyses indicate that the amount of heat produced by the SOFC during the summer exceeds the regeneration heat required by the hybrid desiccant cooling system, leading to substantial surplus waste heat. The lowest waste heat during the summer period is obtained for R1234ze(Z), which has the lowest electricity consumption. This is explained by the fact that the existing SOFC unit operates at a lower capacity, resulting in less waste heat production. Fig. 20 exhibits the temperature variation of the water in the TES unit, which is supplied by the increasing waste heat, for the system using R1234ze(Z) throughout

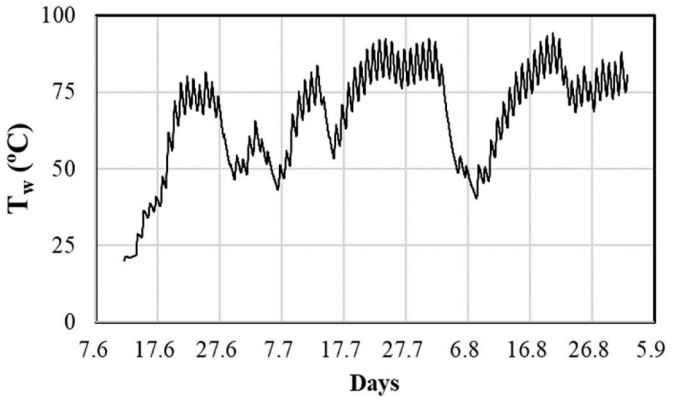

Fig. 20. The variation of average water temperature in the TES unit during the summer period.

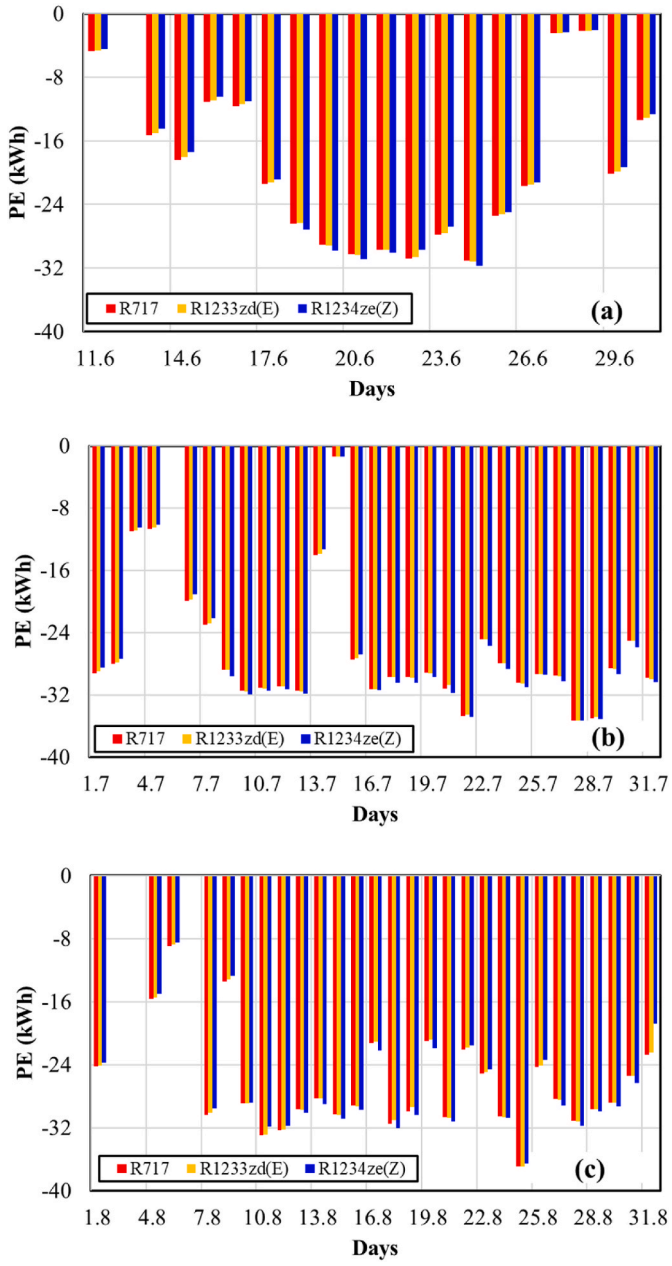

Fig. 21. Primary energy consumption rates for June (a), July (b), and August (c) respectively.

the summer period. To meet the hot water needs for human use, the temperature of the water in the TES unit reached the desired levels (40 °C and above) on June 16th (98 h after the system started). The desired temperatures for using the hot water in the TES unit to balance the regeneration air were reached on June 20th (185 h after the system started), and for the remainder of the period, the temperatures were mostly maintained for balancing the regeneration air. This surplus waste heat in storage TES unit also can be utilized in additional processes such as water heating or laundry drying.

Negative values in primary energy consumption indicate that total heat and electricity production of the system exceeds its consumption (Fig. 21). The amount of electricity produced by the existing SOFC didn't caused the primary energy consumption to drop into the negative because it fully or partially met electricity needs of the cooling system (Fig. 18). However, the SOFC produced more waste heat than needed to generate the desired electricity (Fig. 19). The lowest primary energy consumption was achieved when using R717, which had the highest electrical energy consumption. This is due to its higher demand for electricity and the fact that the SOFC generates more heat energy compared to its electrical energy production. This resulted in the lowest primary energy consumption rates compared to the others. However, since the system has the highest electrical energy consumption and consequently the highest fuel consumption when using R717, it is more suitable to prefer R1234ze(Z) over R717.

Finally, this study compared the primary energy consumption of the system using R1234ze(Z), which has the best performance parameters and consequently the lowest fuel consumption, with and without the SOFC (Fig. 22). In the case without SOFC, it is assumed that natural gas is used to reach the desired temperatures for regeneration air and electricity of the system is supplied from the grid. There is a significant difference (3984.56 kWh) between the primary energy consumption of the desiccant hybrid cooling system operating in combination with the SOFC and without it during the summer period. This energetically demonstrates that desiccant hybrid cooling systems can be used in different configurations with increased future feasibility of SOFC.

Overall, the combination of the SOFC unit, which uses human waste as fuel, with the desiccant hybrid cooling system has provided the following advantages.

- There is no need for additional thermal energy, as the amount of waste heat generated by the condenser and SOFC is sufficient for required regeneration heat of the system.
- The electricity consumption from the grid is reduced, as the existing SOFC system meets a significant portion of the energy demand.
- The system reduces dependency on fossil fuels by using biogas, a renewable energy source.
- The proposed system allows for the utilization of human waste as fuel, offering both the opportunity to meet energy needs and the disposal of these wastes from the environment.

The main disadvantage of the system is that the LHV of human waste, used as fuel, is lower compared to fossil fuels such as natural gas, gasoline, or diesel. As a result, more fuel consumption is required.

5. Conclusions

This study examined the effects of the combined operation of a desiccant hybrid cooling system with an SOFC unit, which uses human waste as fuel, on performance parameters of the system. The following results were obtained within this scope.

- The total compressor power consumption for the entire summer season with R1234ze(Z) was 3.98% and 3.45% lower compared to the cases using R717 and R1233zd(E) refrigerants, respectively. Additionally, except for days with very high ambient temperature and humidity, the compressor power consumption of R1233zd(E) is

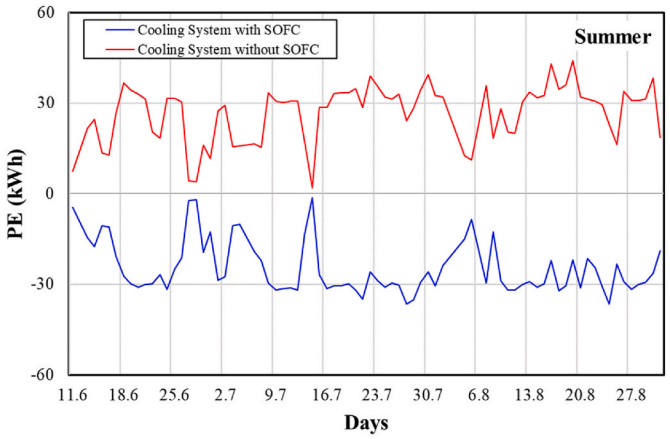

Fig. 22. Comparison of the hourly primary energy consumption of the desiccant hybrid cooling system with and without the use of the SOFC unit.

slightly lower than that of R717. The total energy consumption of the desiccant hybrid cooling system has also shown a similar trend to the compressor power consumption during summer season.

- The heat rejected from the condenser was insufficient to meet the required Regeneration Air Heating (RAH) load in June. However, on days with high cooling loads, the amount of heat rejected from the condenser was sufficient to meet the required RAH load. Therefore, on these days, the heat rejected from the condenser fully covered the RAH load, eliminating the need for an auxiliary heater.
- During the summer period, the existing electricity production from the current SOFC unit met 82.00% of the total electricity consumption of the desiccant hybrid cooling system. Additionally, a significant amount of waste heat is generated during electricity production in SOFC units.
- The total syngas consumption during the summer period was determined to be 12.48 tons for R1234ze(Z). Consequently, the total solid waste requirement reached 15.77 tons. This is 1.19% and 0.90% lower compared to the cases where R717 and R1233zd(E) were used, respectively.
- The highest COP_{el} among the refrigerants was found to be in the system using R1234ze(Z), with an average COP_{el} of 2.05. This is 3.14% and 2.40% higher than the systems using R717 and R1233zd (E), respectively. Additionally, the other COPs considered in this study, COP_{th} and COP_t, were also highest in the system using R1234ze(Z).
- The results showed that during a part of June, the electricity produced by the existing SOFC was mostly sufficient for the desiccant hybrid cooling system. However, on most of the remaining summer days, the electricity demand exceeded the capacity of the existing SOFC unit, necessitating additional electricity from the grid. Compared to the systems using R717 and R1233zd(E), it was determined that the system using R1234ze(Z) achieved additional electricity savings of 9.97% and 9.23%, respectively.
- The SOFC unit produces more waste heat than electricity. Since R717 has a higher electricity demand and consequently higher syngas consumption compared to the others, it resulted in the highest waste heat production. The greater amount of waste heat compared to the others led to R717 having the lowest PE. However, considering fuel and electricity consumption, R1234ze(Z) provided better results. Additionally, it was found that there is a significant difference in primary energy consumption between the desiccant hybrid cooling system operating in combination with the SOFC and the system operating without the SOFC during the summer period.

The proposed system has the potential to reduce dependence on fossil fuels by using biogas, a renewable energy source, and enables the reuse of human waste, allowing for the disposal of these wastes from the environment. Future studies may include testing the system under real climate conditions and validating the presented results.

CRediT authorship contribution statement

Kamil Neyfel Çerçi: Writing – original draft, Visualization, Methodology, Investigation, Conceptualization. **Ivo Rafael Oliveira Silva:** Visualization, Investigation. **Önder Kaşka:** Methodology, Formal analysis. **Kamel Hooman:** Writing – review & editing, Resources, Investigation.

Declaration of competing interest

The authors declare that they have no known competing financial interests or personal relationships that could have appeared to influence the work reported in this paper.

Acknowledgement

We would like to thank the Scientific and Technological Research Council of Türkiye (TUBITAK), International Postdoctoral Research Fellowship Program (TUBITAK 2219) for financially supporting (Grant number:1059B192203025) Dr. Kamil Neyfel Çerçi.

Nomenclature

A	area (m)
c_p	specific heat (kJ/kg)
$\dot{m}$	mass flow rate (kg/h)
$\dot{E}$	Electrical energy rate (kW)
h	specific enthalpy (kJ/kg)
P	pressure (kPa)
ΔP	pressure drop (kPa)
$\dot{Q}$	heat transfer rate (kW)
T	temperature (°C, K)
$\dot{W}$	power consumption rate (kW)

Greek symbols

ε	effectiveness (−)
ω	humidity ratio (g_w/kg_{da})
η	efficiency (% or dec.)
λ	latent heat evaporation (kJ/kg)

Subscripts

aux	auxiliary
o	outdoor ambient
p	process
pa	process air
r	regeneration
ra	regeneration air
RHX	rotary heat exchanger
is	isentropic
mec	mechanic
c,t	total cooling
e	evaporator
cond	condenser
comp	compressor
comp,el	compressor electricity consumption
sen	sensible
l	latent
t	total
th	thermal
el	electrical
RAH	regeneration air heating
reg	regeneration
req	requirement
n,el	net electricity
s	syngas
SOFC	solid oxide fuel cells
s,w	solid waste
h	heating
h,r	heat recovery
h,w	hot water
p	plasma
p,g	plasma gasifier
w	water

Abbreviations

COP	coefficient of performance
VCC	vapor compression cooling unit
DAC	desiccant air cooling unit
DW	desiccant wheel
SOFC	solid oxide fuel cells
RAH	regeneration air heating
PE	primary energy consumption
TES	thermal energy storage unit

Data availability

No data was used for the research described in the article.

References

AlNouss, A., McKay, G., Al-Ansari, T., 2020. A comparison of steam and oxygen fed biomass gasification through a techno-economic-environmental study. Energy Convers. Manag. 208 (October 2019), 112612. https://doi.org/10.1016/j.enconman.2020.112612.

Cavalli, A., Chundru, P., Brunner, T., Obernberger, I., Mirabelli, I., Makkus, R., Aravind, P.V., 2021. Interactions of high temperature H2S and HCl cleaning sorbents with biosyngas main components and testing in a pilot integrated biomass gasifier SOFC system. Renew. Energy 180, 673–682. https://doi.org/10.1016/j.renene.2021.08.114.

Çerçi, K.N., Oliveira Silva, I.R., Hooman, K., 2024. Investigation of the energetic and exergetic performance of hybrid rotary desiccant-vapor compression cooling systems using different refrigerants. Energy 302, 131732. https://doi.org/10.1016/j.energy.2024.131732.

Chen, L., Chu, Y., Deng, W., 2022. Experimental investigation of dedicated desiccant wheel outdoor air cooling systems for nearly zero energy buildings. Int. J. Refrig. 134 (July 2021), 265–277. https://doi.org/10.1016/j.ijrefrig.2021.11.016.

Crawley, D.B., Lawrie, L.K., Army, U.S., Champaign, C., Curtis, I., Pedersen, O., Winkelmann, F.C., 2000. EnergyPlus: energy simulation program. ASHRAE J. 42, 49–56, 10.1.1.122.6852.

Daou, K., Wang, R.Z., Xia, Z.Z., 2006. Desiccant cooling air conditioning: a review. Renew. Sustain. Energy Rev. 10 (2), 55–77. https://doi.org/10.1016/j.rser.2004.09.010.

De Antonellis, S., Joppolo, C.M., Molinaroli, L., Pasini, A., 2012. Simulation and energy efficiency analysis of desiccant wheel systems for drying processes. Energy 37 (1), 336–345. https://doi.org/10.1016/j.energy.2011.11.021.

Delfani, S., Esmaeelian, J., Pasdarshahri, H., Karami, M., 2010. Energy saving potential of an indirect evaporative cooler as a pre-cooling unit for mechanical cooling systems in Iran. Energy Build. 42 (11), 2169–2176. https://doi.org/10.1016/j.enbuild.2010.07.009.

Dong, L., Liu, H., Riffat, S., 2009. Development of small-scale and micro-scale biomass-fuelled CHP systems - a literature review. Appl. Therm. Eng. 29 (11–12), 2119–2126. https://doi.org/10.1016/j.applthermaleng.2008.12.004.

Duffie, J., Beckman, W., 1980. Solar Engineering of Thermal Processes. Wiley.

Erdinc, M.T., 2023. Two-evaporator refrigeration system integrated with expander-compressor booster. Int. J. Refrig. 154, 349–363. https://doi.org/10.1016/j.ijrefrig.2023.06.023.

Fong, K.F., Lee, C.K., 2019. Performance investigation of a SOFC-primed micro-combined hybrid cooling and power system in hot and humid regions. Energy 189, 116298. https://doi.org/10.1016/j.energy.2019.116298.

Fong, K.F., Chow, T.T., Lee, C.K., Lin, Z., Chan, L.S., 2010. Advancement of solar desiccant cooling system for building use in subtropical Hong Kong. Energy Build. 42 (12), 2386–2399. https://doi.org/10.1016/j.enbuild.2010.08.008.

Frein, A., Muscherà, M., Scoccia, R., Aprile, M., Motta, M., 2018. Field testing of a novel hybrid solar assisted desiccant evaporative cooling system coupled with a vapour compression heat pump. Appl. Therm. Eng. 130, 830–846. https://doi.org/10.1016/j.applthermaleng.2017.10.168.

Goel, S., Rosenberg, M.I., Eley, C., 2017. ANSI/ASHRAE/IES standard 90.1-2016 performance rating method reference manual. https://doi.org/10.2172/1398228.

Guo, J., Bilbao, J.I., Sproul, A.B., 2020. A novel solar cooling cycle – a ground coupled PV/T desiccant cooling (GPVTDC) system with low heat source temperatures. Renew. Energy 162, 1273–1284. https://doi.org/10.1016/j.renene.2020.08.050.

Güzelel, Y.E., Olmuş, U., Çerçi, K.N., Büyükalaca, O., 2021. Comprehensive modelling of rotary desiccant wheel with different multiple regression and machine learning methods for balanced flow. Appl. Therm. Eng. 199, 117544. https://doi.org/10.1016/j.applthermaleng.2021.117544.

Güzelel, Y.E., Olmuş, U., Büyükalaca, O., 2022. Simulation of a desiccant air-conditioning system integrated with dew-point indirect evaporative cooler for a school building. Appl. Therm. Eng. 217, 119233. https://doi.org/10.1016/j.applthermaleng.2022.119233.

Haseli, Y., 2018. Maximum conversion efficiency of hydrogen fuel cells. Int. J. Hydrogen Energy 43 (18), 9015–9021. https://doi.org/10.1016/j.ijhydene.2018.03.076.

Heidari, A., Roshandel, R., Vakiloroaya, V., 2019. An innovative solar assisted desiccant-based evaporative cooling system for co-production of water and cooling in hot and humid climates. Energy Convers. Manag. 185 (February), 396–409. https://doi.org/10.1016/j.enconman.2019.02.015.

Islam, M.M., Hasanuzzaman, M., Pandey, A.K., Rahim, N.A., 2019. Modern energy conversion technologies. In: Energy for Sustainable Development: Demand, Supply, Conversion and Management (Issue Ic). Elsevier Inc. https://doi.org/10.1016/B978-0-12-814645-3.00002-X.

Jani, D.B., Mishra, M., Sahoo, P.K., 2018. Performance analysis of a solid desiccant assisted hybrid space cooling system using TRNSYS. J. Build. Eng. 19, 26–35. https://doi.org/10.1016/j.jobe.2018.04.016.

Jia, C.X., Dai, Y.J., Wu, J.Y., Wang, R.Z., 2006. Analysis on a hybrid desiccant air-conditioning system. Appl. Therm. Eng. 26 (17–18), 2393–2400. https://doi.org/10.1016/j.applthermaleng.2006.02.016.

Kays, W.M., London, A., 1984. Compact Heat Exchangers, third ed. McGraw-Hill.

Klein, S.A., 2012. Engineering Equation Solver Academic Professional, V10.442. F-Chart Software.

Klein, S.A., 2017. Trnsys 18: a transient system simulation program. Solar Energy Laboratory 3. The University of Wisconsin: Madison, WI, USA.

Kuo, P.-C., Illathukandy, B., Wu, W., Chang, J.S., 2020. Plasma gasification performances of various raw and torrefied biomass materials using different gasifying agents. Bioresour. Technol. 314, 123740. https://doi.org/10.1016/j.biortech.2020.123740.

Kutlu, C., Erdinc, M.T., Li, J., Wang, Y., Su, Y., 2019. A study on heat storage sizing and flow control for a domestic scale solar-powered organic Rankine cycle-vapour compression refrigeration system. Renew. Energy 143, 301–312. https://doi.org/10.1016/j.renene.2019.05.017.

Liu, M., Woudstra, T., Promes, E.J.O., Restrepo, S.Y.G., Aravind, P.V., 2014. System development and self-sustainability analysis for upgrading human waste to power. Energy 68, 377–384. https://doi.org/10.1016/j.energy.2014.03.005.

Lo Basso, G., de Santoli, L., Paiolo, R., Losi, C., 2021. The potential role of trans-critical CO2 heat pumps within a solar cooling system for building services: the hybridised system energy analysis by a dynamic simulation model. Renew. Energy 164, 472–490. https://doi.org/10.1016/j.renene.2020.09.098.

Masoso, O.T., Grobler, L.J., 2010. The dark side of occupants' behaviour on building energy use. Energy Build. 42 (2), 173–177. https://doi.org/10.1016/j.enbuild.2009.08.009.

Motaghian, S., Rayegan, S., Pasdarshahri, H., Ahmadi, P., Rosen, M.A., 2021. Comprehensive performance assessment of a solid desiccant wheel using an artificial neural network approach. Int. J. Heat Mass Tran. 165, 120657. https://doi.org/10.1016/j.ijheatmasstransfer.2020.120657.

Naqvi, S.R., Jamshaid, S., Naqvi, M., Farooq, W., Niazi, M.B.K., Aman, Z., Zubair, M., Ali, M., Shahbaz, M., Inayat, A., Afzal, W., 2018. Potential of biomass for bioenergy in Pakistan based on present case and future perspectives. Renew. Sustain. Energy Rev. 81 (May 2017), 1247–1258. https://doi.org/10.1016/j.rser.2017.08.012.

Odukomaiya, A., Woods, J., James, N., Kaur, S., Gluesenkamp, K.R., Kumar, N., Mumme, S., Jackson, R., Prasher, R., 2021. Addressing energy storage needs at lower cost via on-site thermal energy storage in buildings. Energy Environ. Sci. 14 (10), 5315–5329. https://doi.org/10.1039/d1ee01992a.

Olmuş, U., Güzelel, Y.E., Büyükalaca, O., 2023. Seasonal analysis of a desiccant air-conditioning system supported by water-cooled PV/T units. Energy Build. 291, 113101. https://doi.org/10.1016/j.enbuild.2023.113101.

Omer, A.M., 2008. Renewable building energy systems and passive human comfort solutions. Renew. Sustain. Energy Rev. 12 (6), 1562–1587. https://doi.org/10.1016/j.rser.2006.07.010.

Ozturk, M., Doğan, B., Erbay, B.L., 2020. Performance assessment of an air source heat pump water heater from exergy aspect. Sustain. Energy Technol. Assessments 42, 100809. https://doi.org/10.1016/j.seta.2020.100809.

Pan, P., Peng, W., Li, J., Chen, H., Xu, G., Liu, T., 2022. Design and evaluation of a conceptual waste-to-energy approach integrating plasma waste gasification with coal-fired power generation. Energy 238, 121947. https://doi.org/10.1016/j.energy.2021.121947.

Roushenas, R., Razmi, A.R., Soltani, M., Torabi, M., Dusseault, M.B., Nathwani, J., 2020. Thermo-environmental analysis of a novel cogeneration system based on solid oxide fuel cell (SOFC) and compressed air energy storage (CAES) coupled with turbocharger. Appl. Therm. Eng. 181, 115978. https://doi.org/10.1016/j.applthermaleng.2020.115978.

Sheng, Y., Zhang, Y., Deng, N., Fang, L., Nie, J., Ma, L., 2013. Experimental analysis on performance of high temperature heat pump and desiccant wheel system. Energy Build. 66, 505–513. https://doi.org/10.1016/j.enbuild.2013.07.058.

Sheng, Y., Zhang, Y., Sun, Y., Fang, L., Nie, J., Ma, L., 2014. Experimental analysis and regression prediction of desiccant wheel behavior in high temperature heat pump and desiccant wheel air-conditioning system. Energy Build. 80, 358–365. https://doi.org/10.1016/j.enbuild.2014.05.040.

Sheng, Y., Zhang, Y., Zhang, G., 2015. Simulation and energy saving analysis of high temperature heat pump coupling to desiccant wheel air conditioning system. Energy 83, 583–596. https://doi.org/10.1016/j.energy.2015.02.068.

Song, J., Sobhani, B., 2020. Energy and exergy performance of an integrated desiccant cooling system with photovoltaic/thermal using phase change material and maisotsenko cooler. J. Energy Storage 32, 101698. https://doi.org/10.1016/j.est.2020.101698.

Tian, S., Su, X., Shao, X., Wang, L., 2020. Optimization and evaluation of a solar energy, heat pump and desiccant wheel hybrid system in a nearly zero energy building. Build. Simulat. 13 (6), 1291–1303. https://doi.org/10.1007/s12273-020-0627-0.

Tian, S., Su, X., Geng, Y., Li, H., Liang, Y., Di, Y., 2022. Heat pump combined with single-stage or two-stage desiccant wheel system? A comparative study on different humidity requirement buildings. Energy Convers. Manag. 255, 115345. https://doi.org/10.1016/j.enconman.2022.115345.

TS-825, Turkish Standard 825, 2013. Thermal Insulation in Buildings. Official gazette, Ankara.

Tu, R., Liu, X.H., Jiang, Y., 2014. Performance analysis of a two-stage desiccant cooling system. Appl. Energy 113, 1562–1574. https://doi.org/10.1016/j.apenergy.2013.09.016.

Yilmaz, T., Erdinç, M.T., 2019. Energetic and exergetic investigation of a novel refrigeration system utilizing ejector integrated subcooling using different refrigerants. Energy 168, 712–727. https://doi.org/10.1016/j.energy.2018.11.081.

Zendehboudi, A., Li, X., 2018. Desiccant-wheel optimization via response surface methodology and multi-objective genetic algorithm. Energy Convers. Manag. 174, 649–660. https://doi.org/10.1016/j.enconman.2018.07.078.